Journal Pre-proof

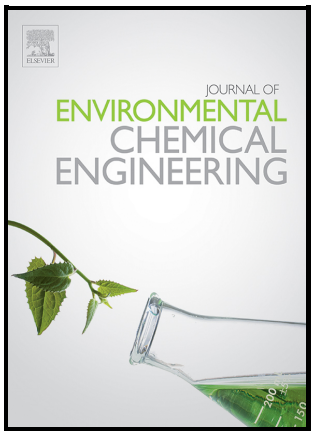

Boosting advanced oxidation processes by biochar-based catalysts to mitigate pesticides and their metabolites in water treatment: a meta-analysis

Jelena Molnar Jazić, Arthur Gross, Bruno Glaser, Jasmina Agbaba, Tajana Simetić, Jasmina Nikić, Snežana Maletić

PII: S2213-3437(24)02391-1

DOI: https://doi.org/10.1016/j.jece.2024.114260

Reference: JECE114260

To appear in: *Journal of Environmental Chemical Engineering*

Received date: 22 July 2024
Revised date: 21 September 2024
Accepted date: 25 September 2024

Please cite this article as: Jelena Molnar Jazić, Arthur Gross, Bruno Glaser, Jasmina Agbaba, Tajana Simetić, Jasmina Nikić and Snežana Maletić, Boosting advanced oxidation processes by biochar-based catalysts to mitigate pesticides and their metabolites in water treatment: a meta-analysis, *Journal of Environmental Chemical Engineering,* (2024) doi:https://doi.org/10.1016/j.jece.2024.114260

Boosting advanced oxidation processes by biochar-based catalysts to mitigate pesticides and their metabolites in water treatment: a meta-analysis

Jelena Molnar Jazić[a], Arthur Gross[b], Bruno Glaser[b*], Jasmina Agbaba[a], Tajana Simetić[a], Jasmina Nikić[a], Snežana Maletić[a]

[a] University of Novi Sad, Faculty of Sciences, Department of Chemistry, Biochemistry and Environmental Protection, Trg Dositeja Obradovića 3, 21000 Novi Sad, Republic of Serbia
[b] Institute of Agricultural and Nutritional Sciences, Soil Biogeochemistry, Martin Luther University Halle-Wittenberg, Halle, Germany
* Corresponding author, E-mail: bruno.glaser@landw.uni-halle.de

Abstract: In order to boost the performance of water treatment in removing organic micropollutants, biochar as an environmental-friendly and sustainable carbonaceous material has been increasingly utilized as a catalyst in advanced oxidation processes (AOP). The main idea behind this research was to unlock the potential of biochar-based catalysts as (i) persulfates and periodate activators and (ii) photocatalyst for mitigating pesticide and intermediate compounds in water treatment. The conducted meta-analysis provides for the first time objective and quantitative overview of the current state of research on biochar-based catalysts application in AOP, surpassing the limitations of conventional qualitative reviews. This paper systematically evaluates the influence of different factors on the weighted degradation efficacy (WDE) achieved by both studied groups of AOP, based on the data extracted from 38 studies conducted in the period 2016-2023. The most of meta-analyzed studies (74%) were published during 2021-2023 covering EU Water Framework Directive priority substances and emerging contaminants. The meta-analysis revealed the high heterogeneity within the results of certain groups ($p=0.05$), indicating the statistically significant influence of the biochar-based catalyst properties, target compound characteristics, pH and water matrix on WDE. The most effective pesticides/intermediate compounds degradation enabled systems containing metal and heteroatom co-doped biochar (e.g. FeS@BC/PMS, S-nZVI@BC/PS) or multicomponent heterojunction (95-99% WDE with 95% confidence interval), and decreased under alkaline conditions and in wastewater. The outstanding catalytic performance of biochar application has been confirmed within the pH 5-8 range, demonstrating significant potential in AOP water treatment.

Keywords: Meta analysis; Persulfates and periodate based AOP; Photocatalysis; Pesticides, Water/wastewater purification

List of abbreviations: AOP - Advanced oxidation processes; WDE - Weighted degradation efficacy; EU WFD - EU Water Frame Directive; EPR - electron paramagnetic resonance; CECs - Contaminants of Emerging Concern; CI - confidence interval; ROS - Reactive oxygen species; SR-AOP - Sulfate radical-based AOP; PI-AOP - Periodate-based AOP; HR-AOP - Hydroxyl radical-based AOP; PS – Persulfate; PDS – Peroxodisulfate; PMS – Peroxymonosulfate; $HO^{\bullet}$ - Hydroxyl radicals; $O_2^{\bullet-}$ - Superoxide radical anions; $HO_2^{\bullet}$- Hydroperoxyl radicals; BC – Biochar; OFG - Oxygen functional groups; nZVI - Nano zero-valent iron; PFR - Persistent free radicals; g-C_3N_4- Graphitic carbon nitride; HA - Humic acid; TOC - Total organic carbon; NOM - Natural organic matter; TMX – Thiamethoxam; BSM - Bensulfuron-methyl; DMM – Dimethomorph; ATZ – Atrazine; 2,4-D - 2,4-dichlorophenoxyacetic acid; γ-HCH – Lindane; QNC – Quinclorac; TCP – Thiacloprid; IMI – Imidacloprid; TCS – Triclosan; MET – Metolachlor; 2,4-DCP - 2,4-dichlorophenol; TZ - 1-H-1,2,4-triazole; 2,4,6-TCP - 2,4,6-trichlorophenol; p-NCB - p-nitrochlorobenzene; PNP - p-nitrophenol; MCB – Monochlorobenzene; 4-CP - 4-chlorophenol; NPA - N-phosphonomethyl iminodiacetic acid; MBZ – Metribuzin; PQT – Paraquat; FRS – Foramsulfuron.

Graphical abstract

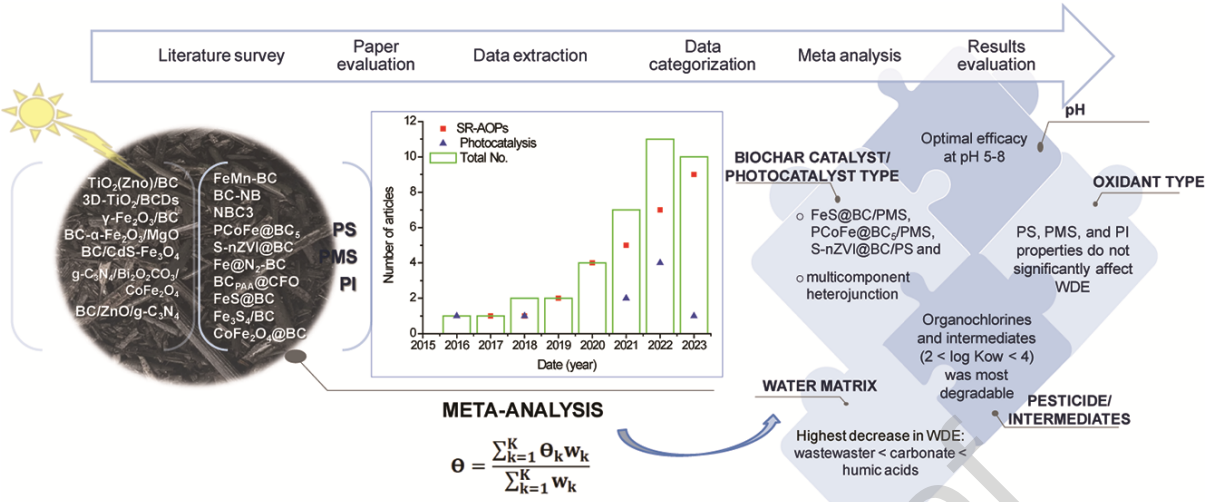

1. Introduction

Recently, advanced oxidation processes (AOP) have gained widespread attention due to their proven ability to degrade contaminants of emerging concern (CEC) and other refractory organic compounds that cannot effectively be removed through conventional wastewater treatment. Among various pollutants, pesticides have revolutionized the agricultural industry while also leaving a significant impact on the global environment due to their widespread residues [1]. Uncontrolled production, storage, and use of pesticides, particularly in low-income countries, may lead to runoff into water bodies, causing contamination of surface water and drinking water sources [1,2]. Pesticides are very challenging to remove during water treatment due to the differences in influent composition, pH and the variability in chemical characteristics of individual pesticides. Poor removal efficacy of pesticides and other CEC might cause their release into the environment, posing contamination risks particularly when effluents are reused for agricultural crop irrigation purposes [3]. Thus, implementation of advanced treatment technologies is necessary in order to cope with hazards to human and environmental health and to prevent drinking water contamination, surpassing the effectiveness of conventional technologies [4-8].

Traditionally, AOP initially investigated in water treatment have relied on the production of reactive oxygen species (ROS) including primarily highly reactive hydroxyl radicals ($HO^{\bullet}$), superoxide radical anions ($O_2^{\bullet-}$) and hydroperoxyl radical ($HO_2^{\bullet}$), that have at least a single unpaired electron involved in oxidation reactions. Among hydroxyl radical-based AOP (HR-AOPs), ozone-based processes, Fenton-based AOPs, and photolytic oxidation have become increasingly investigated for wastewater treatment in recent years [9]. The evolution in the field of AOP resulted in a development of sulfate radical-based AOP (SR-AOP), promoting the generation of sulfate radical ($SO_4^{\bullet-}$), alone or accompanied with $HO^{\bullet}$ [10]. Sulfate radical-based AOP are a revolutionizing and convenient alternative to HR-AOP mainly due to their high oxidation potential (E_0=2.5–3.1 V of $SO_4^{\bullet-}$ vs. E_0=1.8–2.7 V for $HO^{\bullet}$), longer half-life period (30-40 µs vs 20 ns for $HO^{\bullet}$) and possibility of application under wider pH ranges (pH 2-8) with high selectivity and demonstrated fascinating performance [11]. Persulfate (PS) or peroxodisulfate (PDS) and peroxymonosulfate (PMS) are considered to be the most favorable precursors of sulfate radicals applied in water treatment. PS and PMS can be activated by either energy-based processes (UV light, ultrasound, heat) or catalyst-based processes using transition metals and metal oxides, alkaline activation or more recently carbonaceous materials [12]. More novel, periodate (PI)-based AOP (PI-AOPs) exhibited promising future due to the ability to generate more powerful ROS including iodate radicals ($^{\bullet}IO_3$) [13]. Basically, catalytic AOPs utilizing solid catalysts are also categorized as heterogeneous and are used alongside other systems such as persulfates, light, ozone, hydrogen peroxide etc. [14].

Over the past decade, there has been significant interest in utilizing biochar, whether pristine or chemically modified, for AOP-based wastewater treatment of recalcitrant pollutants. This interest stems from its advantageous properties including its expansive specific area, low cost, porous composition, and the abundance of active oxygen functional groups (OFG) on its surface. To accomplish “trash-to-treasure” mission, different types of inexpensive biomass and generally carbonaceous material can be used for the production of biochar by the thermo-chemical conversion

in the presence of limited oxygen supply [15-17]. In addition to animal manure, agricultural, food, poultry residues or any other biomass sources (bamboo, dried leaves, sawdust, fruit seeds), sewage sludge can also serve for the preparation of biochar-based catalysts [18,19]. Thus, biochar is considered as environmental-friendly carbon material that has gained considerable attention in attaining sustainable development goals such as mitigation of climate change, energy production and storage and environmental remediation and water treatment [17,20,21].

Biochar-based metal-free catalysts are eco-friendly promising materials for activation of PS and PMS in water treatment, which empowers overcoming the issues of possible agglomeration and leaching of metals, consequently avoiding secondary water contamination [22-24]. Due to their convenient characteristics, biochar-derived catalysts are able to trigger the cleavage of peroxyl bonds of PS and PMS further leading to the generation of reactive radicals [25]. However, for the specific application, pristine biochar could be affected by inadequate pore size and volume, intermolecular spaces and blocked pores. In order to regulate the biochar structure, including porosity, particle size and surface area, without the additions of chemicals, physical activation can be performed using carbon dioxide or water steam under high temperature, or ball milling approach [26,27]. Morphology regulation of biochar can be tuned through thermal treatment; however, the efficacy of persulfate activation by biochar was not directly correlated to the pyrolysis temperature [28].

To extend the functional properties of pristine biochar as a catalyst support in AOP, chemical modification methods can also be applied resulting in coating, functionalization, impregnation etc. In general, the doping of metals and heteroatoms on biochar serves as a catalytic site, thereby boosting the catalytic activity of modified material toward PS activation [18,26,27]. Non-metallic heteroatom doping involving nitrogen, sulfur, boron and phosphorus is frequently utilized to functionalize biochar through the regulation of its electronic properties further improving adsorptive and catalytic capacity for pollutant removal and degradation in the presence of PS [28-31]. By changing the type of heteroatom, the coordination environment in single-atom catalysts can be improved, enhancing catalyst activity and selectivity. Additionally, BC provides a stable environment for metal coordination, offering a variety of metal active sites for biochar-based single-atom catalysts [32,33].In order to reinforce the separation efficacy of the catalyst for further recycling and biochar reuse, iron-modified biochar has been composed [29,34] whereby the biochar magnetization benefits the recovery of material by external magnetic field [26]. S-doping can improve reactivity, selectivity and stability of nano zero-valent iron (nZVI), reducing adverse side reaction in water. Application of functional composite through multiple modification processes also proved to be an efficient strategy to remove organic contaminants including antibiotics, bisphenols, pesticides, dyes and other CEC from wastewater [35-38]. Alkaline activation of biochar also significantly affects their chemical properties, causing a decrease of acidic functional groups containing oxygen (C=O), enhancing the content of hydroxyl groups on the other side [29], improving the surface properties and increasing the surface area forming new micro- and meso- pores [33,39,40]. Additionally, one of the best collaborative techniques to activate PMS and form additional cavitation centers on carbon-based materials is considered to be ultrasound (US) [41].

In addition to the previously mentioned AOP, photocatalytic processes have also attracted significant attention for organic pollutants degradation in water and wastewater. Biochar has been established as a good carrier for photocatalysis, enhancing the photocatalytic performance of metal oxide or metal [42,43]. Due to its unique characteristics, the application of biochar in photocatalysis has several advantages: it could significantly decrease the recombination rate of electron hole-pairs generated during the photoreaction due to its superior conductive property, prevent metal leaching and enhance photosensitivity and photodegradation on biochar-supported composites under visible light [44,45].

Previously published review articles dealt with the different aspects of biochar-based catalyst application in PS-based AOP focusing on the removal of persistent and emerging organic pollutants from wastewater (e.g. [46,47]) and soil remediation [48]. The significance of biochar-based nitrogen functionalities formation was summarized in-depth, and its application in photocatalysis, electro-catalytic process, and physical adsorption for the remediation of CECs from water was discussed [46]. Ahmad et al. [47] highlighted the role of active radical species in biochar-bases AOP, including photocatalyst, adsorption, electro-Fenton, Fenton-like processes, and catalytic ozonation, for the degradation of persistent pollutants.

There are predominantly qualitative reviews in the field of AOP [e.g. 10,18,19,24,25,47,49,50-57]. Despite the growing emphasis on meta-analysis in the field of emerging substances [58-60], to the best of our knowledge, only three studies performed the meta-analysis to evaluate pesticides removal using AOP. Recent systematic reviews and meta-analysis focused on the organophosphorus pesticides

degradation by electrochemical processes, UV/H_2O_2, photocatalysis, Fenton-based processes, plasma technology, gamma irradiation, sulfate-based catalyst, sonolysis and ozone-based AOP [61], photocatalytic degradation of pesticides [62], and the triclosan removal by SR-AOPs, photodegradation, permanganate oxidation, electrochemical, dechlorination, and adsorption from water [63] evaluating 6-22 studies within meta-analysis. However, none of these papers evaluated the application of biochar-based catalysts in SR-AOP, PI-AOP and photocatalytic processes using the meta-anlysis with quantitative statistical analysis. Tables 1-3 summarize the results of previously published research studies dealing with the degradation of pesticides and its intermediates via biochar-based catalyst activated PS, PMS and PI processes and biochar-supported photocatalyst, highlighting recent progress in this field used for the meta-analysis. This is the first paper specifically focused on novel heterogeneous processes employing biochar-based catalysts for (i) PS or PMS activation (SR-AOP) and PI activation (PI-AOP), and (ii) photocatalysis, using meta-analysis technique to evaluate the process effects on pesticides and their intermediates degradation in water.

Table 1. A review of biochar-based catalysts as activator in SR-AOP and PI-AOP for the free radicals driven pesticide degradation in water.

Table 2. A review of biochar-based catalysts as activator in SR-AOPs and PI-AOPs for the free radicals driven pesticide intermediate compounds degradation in water.

Table 3. A review of biochar-based photocatalysts for degradation of pesticide and its intermediates in water.

The novelty and main strength of the meta-analysis conducted in this research beyond the regular review papers, is that it enables a quantitative and objective statistical analysis of extracted data. This paper offers a strategy for study selection, data extraction and categorization (Section 3.1), which is further used for a comprehensive evaluation within the meta-analysis covering various effects: type of the catalyst (Section 3.2), oxidant type (Section 3.3), pH (section 3.4), characteristics of pesticide/intermediate compounds (section 3.5), light sources (Section 3.6) and water matrix (Section 3.7). Most of the cutting-edge research studies (74%) used for this meta-analysis were published during the last 3 years (2021-2023) covering organic micropollutants of high importance, including the EU Water Framework Directive (2013/39/EU) priority substances (chlorpyrifos, atrazine, lindane) or contaminants of emerging concern listed by the NORMAN Database System (2,4-dichlorophenoxyacetic acid, imidacloprid, triclosan, metolachlor, 2,4-dichlorophenol, 2,4,6-trichlorophenol, 4-chlorophenol, diazinon, glyphosate). This approach enables the assessment of different prospective that might alter the degradation efficacy mediated by radical or non-radical pathways and is additionally summarized in challenges, prospects and future studies recommendations (discussed in Section 3.8).

2. Material and methods

2.1. Literature search approach and data collection

This meta-analysis is based on a comprehensive literature survey conducted using ISI Web of Science, Scopus and Elsevier's Science Direct. The search was conducted using the following keywords: biochar AND advanced oxidation AND pesticide, or biochar AND photocatalysis AND pesticide, with no limitation regarding the publication period. Literature screening process is visualized in Figure 1.

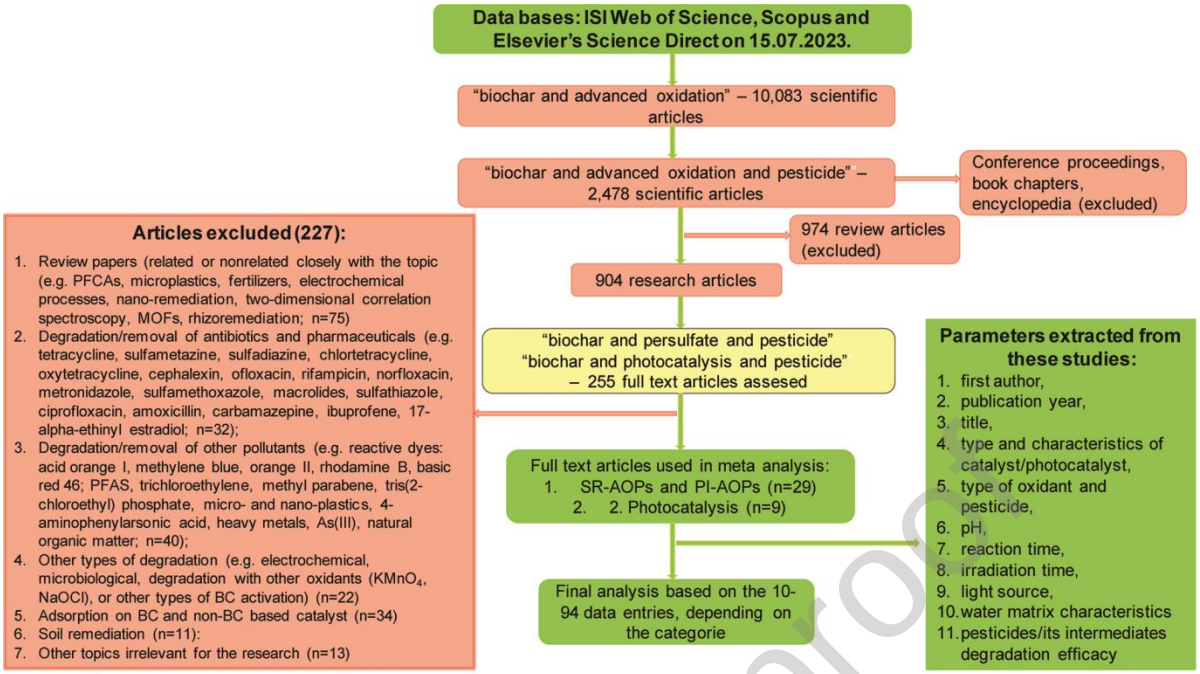

Figure 1. PRISMA diagram - graphic description of the literature search strategy and article selection process for meta-analysis.

The articles have been reviewed by three authors for eligibility. Papers were included in the meta-analysis if they the following criteria:

(1) articles are written in English language as original research paper;
(2) articles are focused on pesticides and their intermediates degradation using biochar or biochar-based catalyst as (i) PS/PMS or PI activator, and (ii) photoactive material for photocatalysis;
(3) articles include complete and relevant information in the selected field.

2.2. Data categorization

Considering the differences in the degradation pathway and mechanism during the SR-AOP or PI-AOP and photocatalysis, meta-analysis calculation and evaluation of the calculated results were conducted separately for both groups of processes. Detailed description of the catalyst characteristics that are evaluated and process parameters are provided in the tables 1-3. The main parameters influencing the efficacy of SR-AOP and PI-AOP were classified into six main groups and further divided into subgroups as given below and were further evaluated in the meta-analysis:

1. *Catalyst type*: (i) pristine biochar derived from spinach remnants, *Acanthopanax senticosus*, sewage sludge, wheat straw, rise husk, commercial biochar (purchased from EGoS), biochar composite derived from Fenton sludge and sewage sludge; (ii) metal or non-metal-doped biochar (CuO/BC; ZVI/BC, nZVI@BC, nZVI/RS, C-nZVI-BC, G-nZVI-BC, BC_{PAA}@CFO, CBC, FeMn-BC; Fe/Mn-SBC, MBM, NBC3); (iii) metal and nonmetal doped BC (Fe@N-BC; S-nZVI@BC, MFB, PCoFe@BC, MNBC, BC-NB).
2. *Oxidant type*: (i) PS, (ii) PMS and (iii) PI;
3. *pH*: (i) ≤5; (ii) 5-8; (iii) ≥9;
4. *Pesticide and its intermediates*: (i) triazine and triazole (atrazine, 1-H-1,2,4- triazole); (ii) neonicotinoids (imidacloprid, thiamethoxam, thiacloprid); (iii) sulfonylurea (bensulfuron methyl); (iv) organochlorine and other chlorinated compounds, Kow>2 (dimethomorph, 2,4-dichlorophenoxyacetic acid, lindane, triclosan, quinclorac, metolachlor); (v) intermediates with one benzene ring, Kow > 2 (2,4,6-trichlorophenol, phenol, p-nitrophenol, monochlorobenzene, 4-chlorophenol, p-nitrochlorobenzene, m-nitrochlorobenzene, o-nitrochlorobenzene);
5. *Water matrix*: (i) synthetic water (deionized/distilled) water; (ii) tap water; (iii) natural waters (river, lake, groundwater); (iv) wastewater; (v) water enriched with chloride (1-10 mM); (vi)

water enriched with nitrate (1-10 mM); (vii) water enriched with hydrogencarbonate (1-10 mM); (viii) water enriched with humic acids (5-10 mg/l); (ix) water enriched with humic acids (10-50 mg/l).

The available data from 9 studies was used to classify the main factors influencing photocatalysis into following groups and corresponding subgroups as described below and were further evaluated:

1. *Photocatalyst type*: (i) pristine (commercial biochar); (ii) metal-doped biochar (ZnO+BC; TiO_2+BC, BC/α-Fe_2O_3/MgO, TiO_2/RHB, 3D-TiO_2/magnetic biochar dots, γ-Fe_2O_3/BC); (iii) metal and non-metal-doped biochar (BC/CdS-Fe_3O_4, BC supported ternary g-C_3N_4/$Bi_2O_2CO_3$/$CoFe_2O_4$ heterojunction, Pbi-ZnO-g-C_3N_4).
2. *pH*: (i) ≤5; (ii) 5-8,5; (iii) ≥9.

Studies included for the meta-analysis of photocatalysis cover various subgroups of pesticide and its intermediates: (i) triazine (atrazine, metribuzin); (ii) organophosphorus (diazinon, N-phosphonomethyl iminodiacetic acid, chlorpyrifos, glyphosate); (iii) sulfonylurea (foramsulfuron); (iv) bipyridylium (paraquat), (v) pesticide intermediate (p-chlorophenol). Considering the small numbers of included available studies and consequently small number of data entries within the diverse subgroups, influence of chemical properties within the specific subgroups were not further evaluated in order to avoid the sample size influence.

Meta-analyzed data on the effects of SR-AOP, PI-AOP, and photocatalysis on the degradation of pesticides/intermediate compounds were compared to the use of separate processes involving adsorption on biochar-based catalyst, application of oxidant alone, or photodegradation in the absence of a catalyst. The impact of the outlined factors on the effectiveness of pesticides and their intermediates degradation efficacy were evaluated under optimal reaction conditions and in synthetic water (deionized or distilled water). Additionally, the effect of pH was evaluated in a wide range to cover acidic, neutral and basic conditions. The influence of water matrix characteristics was estimated for the different water types and in the presence of various interfering species such as organic matter and inorganic ions. If data were not presented in the main text or in supplementary material of the article, WebPlotDigitizer version 4.6 was used to extract values as well as the standard deviation from the figures. Pesticides and its intermediates degradation efficacy (De in %) were taken as a measure of effect size for all studies. Residual concentration of pesticides/intermediates in treated water (Cr) was calculated based on the initial concentration (Ci) and degradation efficacy (De in %) and was further used for the meta-analysis (Equation 1).

$$\mathrm{Cr} = \mathrm{Ci} - \left(\frac{\mathrm{Ci} * \mathrm{De}}{100}\right) \quad (1)$$

2.3. Meta-analysis

For meta-analysis, the individually calculated residual concentration Cr (from now on referred to as "effect size k") of each of the original studies was allocated to a subgroup (specified in chapter 2.2) for further analysis. The pooled effect size result of each subgroup was then calculated using a random effects model. Random effects models utilize the inverse-variance method to calculate a weighting factor w_k assigned to each effect size k, meaning that the uncertainty of each original study (given as standard deviation or standard error) is taken into account in the meta-analysis. Approximately 23% of the included studies lacked of detailed statistical information. Thus, we chose to impute missing standard deviation values using the highest standard deviation of each subgroup dataset, as suggested by Furukawa et al. (2006) [95]. For studies lacking of sample size data, we assigned a default sample size of n=2 to facilitate standard deviation calculations.

Equation 2 describes how the weighting factor *wk* of each original studies' effect size was calculated:

$$\mathrm{w_k} = \frac{1}{\mathrm{s_k^2} + \tau^2} \quad (2)$$

The variance of each individual effect size k is denoted by s_k^2. The Restricted Maximum Likelihood method was used to estimate τ^2 [96]. Subsequently, the weighting factor wk was utilized to determine the pooled effect size for each subgroup, as shown in Equation 3.

$$\Theta = \frac{\sum_{k=1}^{K} \Theta_k w_k}{\sum_{k=1}^{K} w_k} \quad (3)$$

where Θ represents the weighted degradation efficiency for each subgroup, and Θk denotes the weighted degradation efficiency of each individual effect size k. To assess the degree of variation among the original study findings (often referred to as "between study-heterogeneity"), we calculated Cochrans' Q, as specified in Equation 4.

$$Q = \sum_{k=1}^{K} w_k(\Theta_k - \Theta)^2 \quad (4)$$

With Θ indicating the weighted degradation efficiency for each subgroup, Θk representing the weighted degradation efficiency for each individual effect size k, and w_k as the weighting factor for each individual effect size k. Furthermore, to ensure easier interpretation, Higgins and Thompson's I^2 metric was calculated as a percentage to quantify this "between study heterogeneity", as described in Equation 5.

$$I^2 = \frac{Q-(K-1)}{Q} \quad (5)$$

With Q representing Cochrans' Q and K denoting the total number of studies included. Significant differences among group outcomes are noted if the p-value in the table is less than 0.05, calculated using the Q test [97].

For meta-analysis calculation, we employed R Version 4.1.2 [98] along with the "meta" package [77]. The results of the meta-analysis were illustrated using forest plots, with the visualizations also created in R.

3. Results and discussion

3.1. Review of study selection

Insight into the scientific publications in Web of Science, Scopus and Elsevier's Science Direct indicates the increase of scientific interest and research in the field of biochar, with increasing number of publications, starting from 2010 to date, with the total number of publications of 27,132 (ScienceDirect). There has been a significant increase in scientific interest in the field of using biochar and biochar-based materials as catalysts in AOP applied for the water/wastewater treatment. During the last decade, about 10,083 scientific articles contain "biochar and advanced oxidation" and with a more specific application 2478 articles contain "biochar and advanced oxidation and pesticide". After literature screening and exclusion of articles that were not strongly related to the topic, as shown in the PRISMA flow diagram (Figure 1), 29 articles were included in the meta-analysis of the influence of SR-AOP and PI-AOP as well 9 articles in the meta-analysis of photocatalysis effects on the pesticide/its intermediates efficacy. Temporal evolution of the total number of publications that meets the selection criteria are presented in Figure 2, among which the largest number of research articles have bend published during the last 3 years (74%). Finally, the meta-analysis systematically summarized the findings in the investigated field, with a total of 10-94 data entries, depending on the observed group and the processes (section 2.2). Results of the meta-analysis are presented in table 4 and visualized in figures 3-7. Tables 1-3 provides data regarding the catalysts characteristics that are evaluated as well as process conditions with the most important findings of the studies. In the following sections, specific effects on the AOP efficacy will be discussed, emphasizing the most significant variables.

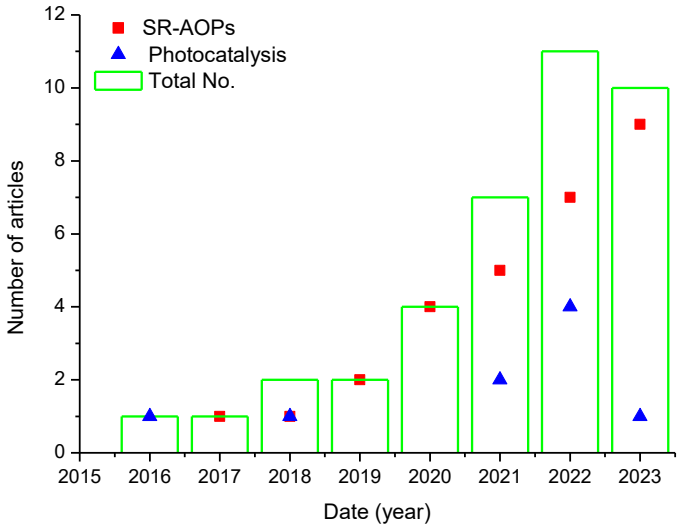

Figure 2. Number of the selected studies reported per year.

3.2. Effect of catalyst type

When biochar was used without the addition of PS or PMS, the reported removal of most investigated pesticides due to adsorption on biochar's surface or/and into its biochar's pores was up to 20%. Slightly higher removal of p-nitrophenol, approximately 30%, was reported as a result of adsorption on modified biochar WSC [85] and C-nZVI-BC and G-nZVI-BC [81] within 600 min. and 90 min, respectively. Additionally, the application of biochar materials enables 46-52% removal of phenolic compounds by adsorption [79,88] and even higher removal rates for nitrochlorobenzene (up to 80%) when reaction time was extended compared to the AOPs [82]. Meta analysis of processed data indicated that application of biochar alone (control treatment) under investigated conditions have no significant impact on the removal of pesticide/intermediate compounds by adsorption from deionized/distilled water (overall removal efficacy was 31%, with high variability within the studies, $p<0.0243$, $n=22$). Additionally, poor degradation removal of the investigated compounds was observed when PS, PMS and PI was used alone (<10%), and were not further proceed for the meta-analysis.

On the other hand, biochar-based catalyst effectively activated PS, PMS or PI, leading to a drastically more effective removal of pesticide/intermediate compounds compared to the application of biochar alone (Figure 3a, table 4). Overall weighted degradation efficacy (WDE) was 92.4% (95% CI = 87.7% to 97.1%, n=31) with a high level of results heterogeneity amongst the articles studied ($p=0.0145$) (table 4). The highest heterogeneity of WDE (95% CI = 78.6% to 100%, $Q=690$) was observed within the subgroup "pristine biochar", prepared by one step pyrolysis of precursor material (table 1), without further addition of chemicals and biochar modification. Despite of high degradation efficacy, pristine biochar might exhibit poor catalytic activity toward PS activation due to its unstable performance and sp^2-hybridized carbon framework, requiring the application of different modification methods to improve its catalytic performance [30,31].

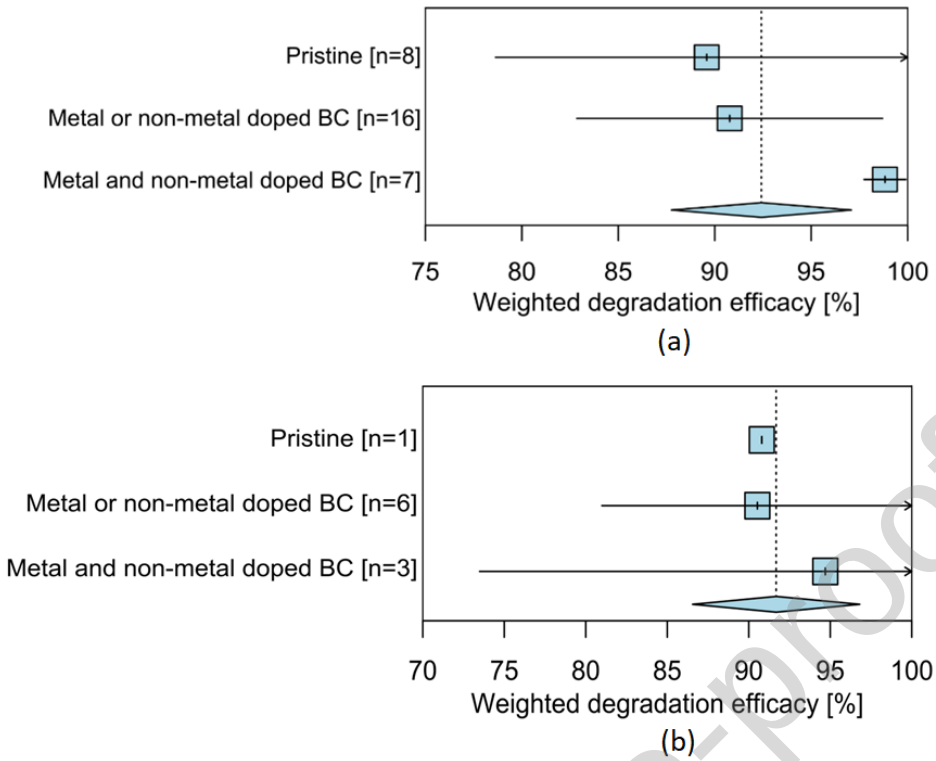

Figure 3. Forest plot of the effects of the catalyst type on weighted efficacy of pesticide/intermediate compounds degradation during the (a) SR-AOPs and PI-AOPs and (b) photocatalysis, based on the random effects model (CI = 95%) of the average effect size. The vertical black dotted line represents the mean overall degradation efficacy (%) per category. Blue squares indicate the mean degradation efficacy per subgroup. Each effect size is presented as the range between the upper and lower 95% confidence interval. The extend of the blue rectangle represents the confidence interval of the overall degradation efficacy. Group category names are presented on the y-axis black letters. The number of included treatments is given in brackets.

Subgroup analyses revealed that systems with biochar catalyst doped with metal and nonmetal were slightly more effective in pesticide/intermediate compounds degradation (99% WDE) compared to the one step modified biochar catalyst with metal or nonmetal content or pristine BC (about 90% WDE). Relatively high I^2 value in all subgroups (71-99%) indicates substantial heterogeneity between individual studies. Obtained results indicate that biochar, doped with metal and/or nonmetal has a synergistic effect on the activation process of PS or PMS and PI compared to the control treatment. For example, available data indicate that one step biochar modification with the N-doping method enhances the electron transfer within the carbon skeleton and charge density of carbon atoms [16,28,31]. Four typical N-doping configurations including pyridinic, graphitic, pyrrolic nitrogen as well as and oxidized nitrogen were observed as a result of biochar modification and were responsible for dimethomorph and bensulfuron methyl degradation [16,31,99]. Zero valent iron and biochar composite can improve PS activation and the generation of free radicals accompanied with the changing of iron valence state [34,72]. Similarly, Fe-Mn bimetallic catalysts have better PC activation performance compared to the corresponding monometallic oxides for thiamethoxam degradation [30]. Generally, complex metal radical complexes on the biochar surface called persistent free radicals (PFR) have a strong electron transfer capability and can cause the formation of ROS by transferring electrons to oxygen, hydrogen peroxide and PS, thus participating in the degradation process. Furthermore, accompanied transition metals and polyacrylic acid-modified biochar quickly activate PMS and provide high efficacy for the quinclorac degradation [36]. However, Hayat et al. (2020) observed that CuO/BC did not increase PS activation efficacy compared to the CuO alone for the degradation of imidacloprid in water [73].
Results of our meta-analysis revealed that systems within the metal and non-metal co-doped biochar catalysts subgroup showed the highest degradation efficacy for the investigated pollutants (95% CI = 97.7% to 99.9%) and were as follows: MFB-500/PMS and PCoFe@BC_5/PMS for the 2,4-D

degradation [66,70], S-nZVI@BC/PS for the ATZ degradation [67], Fe_3S_4/BC/PMS for the 2,4,6-TCP degradation [37], Fe@N_2-BC900/PS for the γ-HCH degradation [68], $MNBC_{800}$/PMS for the MET degradation [75] and BC-NB900/PDS for the BSM degradation [31]. Multiply modified biochar composites that have been analysed contain up to 50% Fe, 8.5% P, 2.18% Co, 5.31% N, 34.3% S and 8.5% B that are along with the carbon and oxygen involved in the reactions on the biochar surface and degradation mechanism. Lowest level of heterogeneity between studies was observed for subgroup 3, additionally confirmed by the lower Q value (Table 4).

Table 4. Results of the meta-analysis of investigated AOPs

Photocatalysis, a process that utilizes light energy to generate electron-hole pairs that can participate in redox reactions, has initially employed titanium dioxide and zinc oxide. Recently it was noted that functionalized biochar can efficiently degrade organic pollutants via redox reactions involving $O_2^{\bullet-}$, $HO^{\bullet}$ and $^1O_2$ and through physical adsorption and chemical interactions [53,100]. It was also established that biochar matrix enhances visible light absorptivity power, and strengthens other nanocatalysts, captures impurities on its surface, and slows the rapid recombination of electron-holes, thereby boosting the photocatalyst's effectiveness [101].

Results on photodegradation evaluated in our study revealed that paraquat, glyphosate, foramsulfuron and diazinon were highly stable under irradiation [88,91-93], while adsorption plays an important role in the removal of organic pollutants during the photocatalysis [89,92]. The results of our meta-analysis of photocatalytic degradation process employing the different biochar-supported photocatalysts are visualized in figure 3b. The overall WDE during the photocatalysis was 91.8 (95% CI: 85.9–97.6, n=10), with the low level of heterogeneity among the studied articles within the group ($p>0.726$). No significant difference in WDE among the subgroups was observed, indicating high degradation efficacy for both commercial biochar and BC-based composites. The broader confidence interval of metal and non-metal-doped biochar can be attributed to the relatively low number of observations (n=3) where heterogeneity may be a result of sampling error.

Obtained results revealed that slightly higher pesticides degradation was achieved using biochar heterojunction including graphitic carbon nitride (g-C_3N_4) and metal oxides (94.7% WDE) compared to the biochar catalysts modified solely with metal oxides (e.g. γ-Fe_2O_3/BC, TiO_2/BC) or commercial biochar alone (91% WDE). Improved photocatalytic performance of composite materials (e.g. BC/CdS-Fe_3O_4, BC supported ternary g-C_3N_4/$Bi_2O_2CO_3$/$CoFe_2O_4$ heterojunction) can be attributed to the synergistic effects of biochar and metal oxides [45,92]. Previously, it was well established that despite the high photostability and non-toxic properties of commonly used metal based photocatalysts, such as TiO_2, ZnO, RuO_2, SiO_2, ZrO_2, CdS, and ZnS, these materials encounter some challenges such as high band gap energy, rapid electron–hole (e^--h^+) pair recombination, poor response to visible light and tendency towards aggregation and agglomeration, reducing their reactivity [76,102,103]. Combining biochar with such photocatalytic materials can create synergistic effects, whereby the porous structure and functional groups present in biochar can enhance the stability and activity of the photocatalyst by providing sites for catalyst deposition and promoting electron transfer during photocatalysis [89,104-106]. For example, BC/CdS-Fe_3O_4 nanocomposite provided excellent photocatalytic properties for the chlorpyrifos degradation due to the improved e^--h^+ separation produced by CdS and the inhibition of nanostructure agglomeration, further enabling separation of catalyst by the magnet. Moreover, biochar-based heterojunction structured photocatalysts, comprising of two or more semiconductor materials might offer more suitable band gaps and energy band structures, enhancing light trapping capabilities for the photocatalysis [107-112].

For instance, the enhanced photocatalytic efficiency of BC-α-Fe_2O_3/MgO composite is attributed to the formation of a heterojunction between α-Fe_2O_3 and MgO, promoting the generation of $HO^{\bullet}$ and $O_2^{\bullet-}$ for the N-phosphonomethyl iminodiacetic acid degradation [89,90]. Biochar supported ternary g-C_3N_4/$Bi_2O_2CO_3$/$CoFe_2O_4$ heterojunction enables effective 4-nitrophenol removal under visible light due to the lower band gap and higher adsorption potential enabling simultaneous adsorption and photocatalytic degradation. Reactive species $HO^{\bullet}$ and $O_2^{\bullet-}$ have been involved in the photo-catalyzed degradation of 4-NP [92]. Generally, the results of our meta-analysis confirmed that biochar-based catalyst can be applied effectively in both SR-AOP, PI-AOP and photocatalysis for the degradation of pesticides and intermediate compounds.

3.3. Effect of oxidant type

PS (E_0 = 2.0 V) and PMS (E_0 = 1.4 V) are among the strongest oxidizing agents that can be applied in water treatment and environmental remediation. However, the most important oxidizing species required for the pollutant degradation are radicals formed upon cleavage of the peroxide O-O bond including sulphate radicals (E_0 = 2.5-3.1 V) and hydroxyl radicals (E_0 =1.8-2.7 V). PMS has a shorter bond length (0.146 nm) and requires higher bond dissociation energy (377 kJ mol^{-1}) for the homolytic cleavage than PS (140 kJ mol^{-1}) [112,113]. PI as new precursor for the generation of ROS with an oxidation potential of E_0 = 1.6 V, can be activated similar as PS and PMS by certain catalysts (e.g. transition metals), microwave, ultrasound and carbon-based materials including biochar, additionally producing novel free radicals including $IO_3^{\bullet}$, $IO_4^{\bullet}$ and $O(^3P)$ [114]. The functional groups of carbonaceous materials that possess oxygen (especially the carbonyl group) act as the active sites involved in mediating electron transfer, effectively contributing to the PS and PMS activation [113], [115] and more novel activation of PI [13]. For example, generation of $SO_4^{\bullet-}$ and ROS on the biochar surface through PS activation can be described by the following equations (6-8) [47]:

$$Biochar_{surface}\text{-}OH + S_2O_8^{2-} \rightarrow Biochar_{surface}\text{-}O^{\bullet} + SO_4^{\bullet-} + HSO_4^{-} \quad (6)$$
$$Biochar_{surface}\text{-}OOH + S_2O_8^{2-} \rightarrow Biochar_{surface}\text{-}OO^{\bullet} + SO_4^{\bullet-} + HSO_4^{-} \quad (7)$$
$$SO_4^{\bullet-} + OH^{-} \rightarrow HO^{\bullet} + SO_2^{-} \quad (8)$$

Activation of PMS and PS can effectively be enhanced by the carbon-based materials doping with heteroatoms, especially nitrogen, due to its comparable atom size and strong bonding with carbon [116]. Additionally, in the presence of metal components on the biochar surface, PS or PMS has the capacity to accept an electron from a transition metal (M) and produce sulphate radicals (Eqs. 9-11), initiating degradation process [47]:

$$Mn^{+} + S_2O_8^{2-} \rightarrow SO_4^{\bullet-} + SO_4^{2-} + Mn^{(n+1)+} \quad (9)$$
$$Mn^{+} + HSO_5^{-} \rightarrow SO_4^{\bullet-} + OH^{-} + Mn^{(n+1)+} \quad (10)$$
$$Mn^{(n+1)+} + SO_4^{\bullet-} \rightarrow SO_4^{2-} + Mn^{+} \quad (11)$$

Summarized effects of oxidant type (PS, PMS and PI) on the pesticide/intermediate compounds degradation using biochar-catalyst mediated AOP are visualised in Figure 4. Presented results of the meta-analysis indicate that biochar-based catalyst showed high efficacy in activating PS, PMS and PI (overall WDE>90%) with no significant influence between the type of the applied oxidant (p=0.1979). Slightly higher level of results variability was observed within the articles that investigated the application of PMS (95% CI = 77.9% to 100%, n=11) than PS (92% CI = 85.1% to 98.1%, n=11), which is also indicated by the higher Q and I^2 values for PMS (table 4).

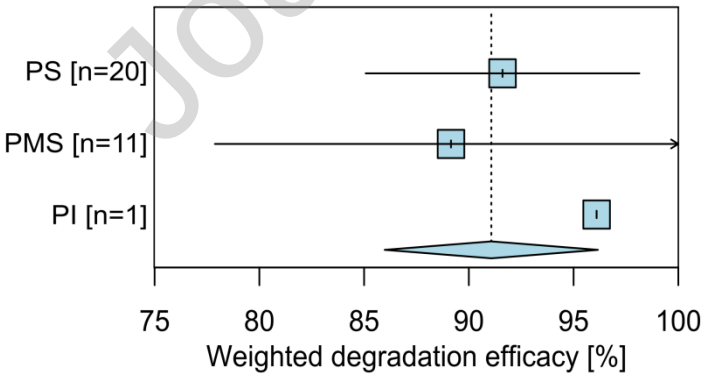

Figure 4. Forest plot of the oxidant type (persulfate-PS, peroxymonosulfate-PMS or periodate-PI) effects on the activation by biochar-based catalyst and subsequent weighted degradation efficacy of pesticide/intermediate compounds, based on the random effects model (CI = 95%) of the average effect size. The vertical black dotted line represents the mean overall degradation efficacy (%) per category. Blue squares indicate the mean degradation efficacy per subgroup. Each effect size is presented as the range between the upper and lower 95% confidence interval. The extend of the blue rectangle represents the confidence interval of the overall degradation efficacy. Group category names

are presented on the y-axis black letters. The number of included treatments is given in brackets.

Authors of studies included in the meta-analysis (table 1 and 2) indicate that using PS/PMS or PI alone without catalysts, negligible degradation of the target pollutant occurs. Table 5 presents the main reactive species formed during SR-AOP and PI-AOP, along with the degradation pathways (discussed in section 3.5). Quenching tests were conducted using methanol, ethanol, tert-butyl alcohol, isopropyl alcohol, furfuryl alcohol, L-histidine, benzoquinone, sodium azide. Quenching experiments, accompanied by electron paramagnetic resonance (EPR) detection, are essential for exploring the role of reactive species and the degradation mechanism. For instance, methanol can quench both $HO^{\bullet}$ and $SO_4^{\bullet-}$, while $HO^{\bullet}$ is preferentially quenched by *tert*-butanol with much higher reaction kinetic than $SO_4^{\bullet-}$. Additionally, benzoquinone and L-histidine are commonly used to determine $O_2^{\bullet-}$ and $^1O_2$ species.

Table 5. Summary of pesticides and intermediate compound degradation mechanism and pathways during the biochar-based catalysts AOPs

Specific quenching tests and EPR revealed that PS and PMS activation by biochar generates $SO_4^{\bullet-}$, $HO^{\bullet}$ and $O_2^{\bullet-}$, as the dominate reactive free radicals, while $^1O_2$ and electron transfer also contributed in the non-radical degradation pathway of pesticides/intermediate compounds. The predominance of the main reactive species, and accordingly the radical or non-radical degradation pathway, depends on the applied system. Additionally, He et al. (2022) indicated the formation of $IO_3^{\bullet}$ and $HO^{\bullet}$ during the PI activation by Fe/Mn-SBC system that effectively degrades thiacloprid in water [69]. Presented results suggest that under optimized reaction conditions, all investigated oxidants (PS, PMS and PI) can effectively be activated in the heterogeneous system, leading to the high degree of pesticide/intermediate compounds degradation in water.
Moreover, novel study by Nan et al. (2024) revealed that ball-milling treatment boosted the ability of biochar for electron transport, thereby enhancing its properties to activate PDS for the tetracycline hydrochloride degradation. Increasing in ball-milling time improved the biochar catalytic ability toward antibiotic degradation, highlighting the potential of this approach to enhance catalyst properties and its application in wastewater treatment [27].

3.4. Effect of pH

pH is one of the most important factors that influence activation efficiency of oxidants by carbon-based (nano)materials. pH of the solution affects the speciation of the target pollutant, the form of the applied oxidant and the surface charge of biochar-based catalyst, additionally influencing the generation and speciation of reactive oxidizing species during the heterogeneous AOP. Thus, dissociation constants of target pollutant as well as the catalyst point of zero charge should be considered in order to achieve effective oxidative degradation [18].
The results of our meta-analysis based on the 95 data entries within the group indicate the high influence of pH on the pesticide/intermediate compounds degradation during the SR-AOP or PI-AOP heterogeneous systems (Figure 5a, table 4). Overall WDE was 79% (95% CI = 74% to 84%, n=95) with a high level of results variability within the group (p=0.0207). The most effective pesticide/intermediate compounds degradation during the analysed SR-AOP or PI-AOP systems was established within pH 5-8 range and in acidic (pH<5) conditions (82.4-85.9% WDE, n=31). Analysed results also suggest that the degradation efficacy of the investigated compounds decreased with increasing pH (95% CI = 59.1% to 79.7%, n=33) within the subgroup pH≥ 9.

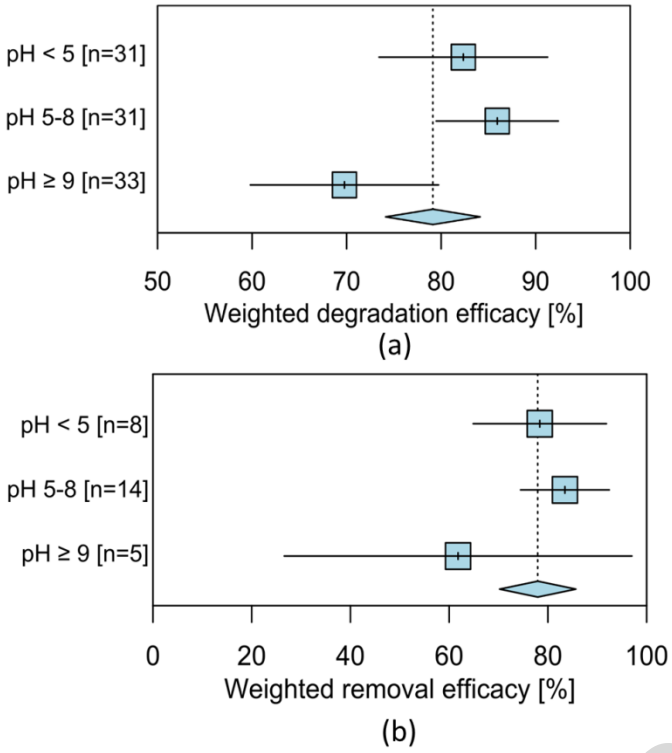

Figure 5. Forest plot of the pH effects on the weighted degradation efficacy of pesticide/intermediate compounds during the (a) SR-AOPs or PI-AOPs systems and (b) photocatalysis, based on the random effects model (CI = 95%) of the average effect size. The vertical black dotted line represents the mean overall degradation efficacy (%) per category. Blue squares indicate the mean degradation efficacy per subgroup. Each effect size is presented as the range between the upper and lower 95% confidence interval. The extend of the blue rectangle represents the confidence interval of the overall degradation efficacy. Group category names are presented on the y-axis black letters. The number of included treatments is given in brackets.

Our meta-analysis revealed low level of heterogeneity between the results of photocatalytic pesticides degradation under different pH (overall WDE 79%, p=0.2466, n=27) (Figure 5b, table 3). The most effective photodegradation of pesticide/intermediate compound (WDE of 83%, n=15) occurred within the pH range of 5<pH<8.5. Moreover, our meta-analysis indicates decreasing photodegradation efficacy with increasing of pH, with a WDE of 62% (95% CI = 27% to 97%, n=5) observed at pH≥ 9. The highest level of heterogeneity within the studies was observed under alkaline conditions, based on the Q an I^2 values.

Generally, biochar-based catalysts showed a stable performance over a wide pH range of 3-10 (e.g. [16,30,31,67,69,71], however, the efficacy of certain catalysts significantly dropped in the alkaline (pH>9) [49,53] as well as strong alkaline and acidic conditions (3>pH>9) [71,75]. Acidic conditions cause a protonation of catalyst surface [66,117] and favour metal ions leaching from the catalyst. Li et al. (2022a) indicates that the highest removal efficacy of QNC achieved at pH 4 can be attributed to the eroded material surface that enables more conducive reaction of Fe^{2+} and Co^{2+} with PMS [36]. Easy entry of iron into aqueous solution under acidic conditions promotes the degradation reactions and catalytic efficacy for thiamethoxam removal [30]. Decomposition of oxidants is also pH-dependent, where acidic conditions are more favourable for the decomposition of PS and generation the sulphate and hydroxyl radicals (Eq. 12) [30,64,118,94]. However, the high concentration of protons can convert the generated $HO^{\bullet}$ and $SO_4^{\bullet-}$ into ineffective H_2O and HSO_4^- [71]. Furthermore, low degradation rate of certain pollutants in strong alkaline conditions are attributed to the increase of electrostatic repulsion between the catalyst surface and PS/PMS [31]. Additionally, electrostatic repulsion between the pesticides (e.g. triclosan, 2,4-D) and biochar catalyst might hinder the interactions causing the depression of the catalytic efficacy [66,71,74]. The strong alkaline environment also reduces the degradation efficacy due to the: (i) quenching reactions of OH^- with ROS in the system (e.g. Eq. 13) and (ii) decomposition of PMS (*pKa*=9.4) into ineffective form of

SO_4^{2-} and H_2O (Eq. 14) [71,74,75].

$$S_2O_8^{2-} + H^+ \rightarrow HS_2O_8^- \rightarrow SO_4^{2-} + SO_4^{\bullet-} + H^+ \quad (12)$$
$$SO_4^{\bullet-} + OH^- \rightarrow SO_4^{2-} + HO^\bullet \quad (13)$$
$$HSO_5^- + SO_5^{2-} + OH^- \rightarrow 2SO_4^{2-} + O_2 + H_2O \quad (14)$$

High degradation efficacy of biochar-based catalysts in heterogeneous AOP under extensive pH conditions enhances the application potential of biochar in water/waste water treatment. Application of heterogeneous AOP at neutral and weak acidic/basic conditions prevents secondary pollution of water and simultaneous degradation of catalyst stability which might occur under the strong acidic conditions, providing an environmentally friendly technique with recovery of catalysts for different purposes.

pH is also one of the most significant factors in the photocatalytic process, since it affects the surface charge and characteristics of a catalyst, further influencing the generation of hydroxyl radicals and the formation of positive charges. Reaction between hydroxyl ions and positive charges on the supported catalyst are strongly pH-dependent and affect the pesticide degradation [103].

The maximal pesticides degradation efficiency typically occurs when the pH of water matrix is between the values of pKa and the point of zero charge of the catalyst. Within this range, the positively charged surface of the photocatalyst can attract and adhere to the negatively charged form of pesticides, contributing to a higher breakdown rate of pesticides [62,119,120].

Analyzed studies indicate the significant drop in degradation efficacy under alkaline [88,93] and acidic conditions [45,88]. Kumar et al. (2018) observed that highest paraquat degradation by ternary g-C_3N_4/$Bi_2O_2CO_3$/$CoFe_2O_4$ heterojunction occurred in pH range 5-7 and falls at highly basic and acidic conditions [93]. Maximal photodegradation efficiency of diazinon and chlorpyrifos occurred at pH 8-9 due to electrostatic interaction between the catalyst surface and pesticides and high production of hydroxyl radicals [45,88]. In contrast, Le et al. (2021) observed that the photodegradation efficiency of glyphosate was up to 99% after irradiation at pH 3 with a TiO_2/RHB with the point zero charge suitable for glyphosate removing [92]. In summary, high WDE achieved under pH close to neutral indicates the high potential of photocatalysis processes in real water treatment conditions.

3.5. Effect of pesticides/intermediate compounds characteristics

Results of our meta-analysis indicate a significant impact of chemical properties of pesticides and intermediate compounds on the degradation process when biochar-based materials were used to activate PS, PMS and PI ($p=0.0385$) (Figure 6). The lowest level of results variability was observed within the oxidative degradation of organochlorine pesticide and intermediates (93.4-96.8% WDE), compounds with mediate level of hydrophobicity ($2 < \log K_{ow} < 4$), that proved to be the most susceptible to degradation. Highest variability of the results was observed for the degradation of neonicotinoids, that have the lowest $\log K_{ow}$ among investigated compounds, ranging from $\log K_{ow}$ of -0.13 (thiamethoxam) to $\log K_{ow}$ of 1.26 (thiacloprid). Additionally, thiamethoxam was the least prone to degradation during the CuO/BC-SPS system [73] compared to the degradation of other investigated pesticides and their intermediates by SR-AOPs. A recent study by Erdem and Erdem (2024) indicates that general approaches for sorption processes can also be implemented for heterogeneous radical-based oxidative systems. In line with their findings, our research also confirmed that compounds with moderate adsorption potential can be efficiently removed during the SR-AOPs and photocatalysis [121].

Under the optimal reaction conditions, almost similar overall weighted degradation efficacy of pesticides and intermediates was observed during the photocatalysis using biochar composites (91.8%) and previously discussed SR-AOP or PI-AOP (92.5%). Results of our meta-analysis showed the high variability of results within the group regarding the photocatalytic degradation ($p=0.0083$). Due to the low number of analysed available studies within the different pesticide classes including triazines (n=2), sulfonylurea (n=1), organophosphorus (n=4), bipyridylium herbicides (n=1) and intermediate (n=1), influence of chemical properties within the subgroups were not further evaluated in order to avoid the sample size influence.

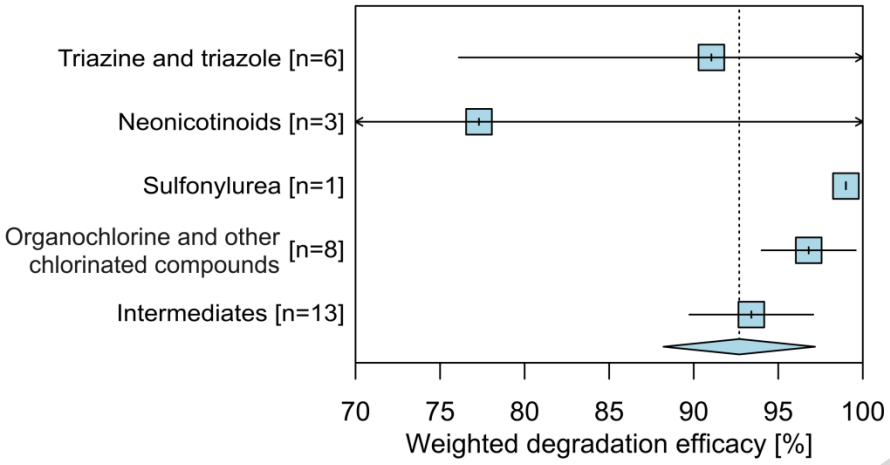

Figure 6. Forest plot of the influence of pesticide and its intermediates characteristics on the weighted degradation efficacy of pesticide/intermediate compounds during the SR-AOP or PI-AOP systems, based on the random effects model (CI = 95%) of the average effect size. The vertical black dotted line represents the mean overall degradation efficacy (%) per category. Blue squares indicate the mean degradation efficacy per subgroup. Each effect size is presented as the range between the upper and lower 95% confidence interval. The extend of the blue rectangle represents the confidence interval of the overall degradation efficacy. Group category names are presented on the y-axis black letters. The number of included treatments is given in brackets.

The degradation pathways of the investigated contaminants under different biochar-based systems are summarized in Table 5 (where data has been available). The extracted data provide an overview of the main reactive species involved in the degradation and main chemical mechanism that took place during the degradation. The degradation pathway depends on the chemical structure of target pollutants as well as the applied BC-based system. Among the available findings, the degradation of atrazine is the most studied. For instance, the degradation of atrazine may occur mainly via radical or non-radical pathways, as confirmed by the detected transformation intermediated. Generally, atrazine is subjected to alkyl-oxidation, dealkylation, dechlorination, leading to ring cleavage and mineralization. Based on the provided m/z values, some of the identified intermediates that are common to different systems are 2-hydroxy-4-ethylamino-6-isopropylamino-s-triazine (m/z 198), 2-hydroxy-4-acetamido-6-isopropylamino-s-triazine (m/z 212), 2-chloro-4,6-diamino-s-triazine (m/z 146), 2-hydroxy-4,6-diamino-s-triazine (m/z 128). Furthermore, predominance of $SO_4^{\bullet-}$/$HO^{\bullet}$ or $HO^{\bullet}$/$IO_3^{\bullet}$ radicals lead to the different degradation mechanism of neonicotinoids, which vary between SR-AOP and PI-AOP. Degradation process of organochlorine and other chlorinated compounds (logKow>2) DMM, 2,4-D, TCS and MET mainly included hydroxylation, decarboxylation, dechlorination and dealkilation. The proposed mechanism for intermediate compound degradation eventually leads to ring opening, formation of small molecular carboxylic acids, and mineralization. Finally, apart from atrazine, there are no multiple degradation studies available for other pesticides or intermediates using different BC-based catalyst AOP, the available data are scarce.

3.6. Effect of light source

The efficiency of pesticide breakdown can be impacted by the light source applied in photocatalysis. For instance, many catalysts can only be activated by UV light due to their high band gap energies thereby limiting wider utilization of visible and sunlight for photocatalytic purposes [122-124]. To address this gap, attention has been devoted to the development of binary or ternary heterojunction-based photocatalysts in which additional semiconductor components are introduced to enhance the separation of charge carrier and increase sunlight absorption [89,108,112,125].
Studies subjected to our meta-analysis covered photocatalysis conducted under simulated solar lights with a xenon light source (35-220 W) [77,89,90,91,93], sunlight [88], visible LED light (60W) [45] and UV light with a maximum emission at 365 nm [91,94]. Among artificial light sources, xenon lamps provide the most faithful reproduction of the solar energy distribution in the wavelength region 290-700 nm with a maximum intensity at wavelengths above 400 nm. Irradiation time required to

achieve maximal degradation efficacy varied from 40-300 min. depending on the catalyst type, light source and compound characteristics.
Specific quenching tests and EPR analysis revealed that biochar-based catalysts, upon irradiation, produce holes, electrons, $SO_4^{\bullet-}$, $HO^{\bullet}$, $O_2^{\bullet-}$ and $^1O_2$ (table 5). Our meta-analysis indicates the low level of results heterogeneity within the group (p=0.1988). High degradation efficacy indicates that investigated photocatalyst including multicomponent heterojunction can efficiently absorb sunlight, particularly visible light, exhibiting high photocatalytic activity (92% WDE). Biochar proved to be a good carrier for photodegradation processes under solar light, improving the catalytic activity and enabling utilization of solar energy. Considering that the most of studied photocatalysts were activated under simulated or natural solar light, and only two studies cover activation under UV-A light, the influence of light source within the specific subgroups were not further discussed.

3.7. Effect of water matrix

The water matrix also might have a significant influence on the overall degradation efficacy during the AOP. Natural organic matter derived from groundwater and surface water and organic matter present in wastewater can scavenge the reactive radical species, remarkably inhibiting their generation and further reducing the degradation efficacy. Some anions present in natural waters (chloride, carbonate, nitrate, sulfate) also compete with target pollutants toward ROS, producing species with the weaker oxidation ability [4,75]. Based on the analyzed data, it was determined that water matrix characteristics have a significant influence on the degradation efficacy of pesticide/indermediate compounds during the SR-AOP or PI-AOP heterogeneous systems (Figure 7, table 4). A high level of results variability within the group was observed (p=0.0016) with the overall WDE of 80.6% (95% CI = 75.7% to 85.5%, n=94). The lowest level of results variability was obtained during the AOP treatment of deionized/distilled water in the absence of interfering ions, with the highest WDE of 93.3% (95% CI = 89.3% to 97.4%, n=32). Results of our meta-analysis revealed that wastewater has the most pronounced influence on the pesticide/indermediate compounds degradation by the SR-AOP or PI-AOP heterogeneous systems, followed by the water containing hydrogen carbonate (1-10 mM) and humic acids (10-50 mg/l HA). Within the group, WDE ranged in the following order: wastewaster (62.3%) < carbonate-containing water (66.0%) < high concentration of humic acids (70.9%).
Investigated wastewater has a high organic load based on the total organic carbon content (up to 1106 mg/L TOC) and chemical oxygen demand (up to 344.8 mg/L COD) as well as high inorganic content (e.g. up to 1496 mg/L chloride; 909.8 mg/L nitrate) [64,75]. Degradation of atrazine, metolachlor, triclosan, and intermediate compounds from pesticide production (4-chlorophenol and 2,4-dichlorophenol) during the heterogeneous SR-AOP was greatly inhibited in wastewater, requiring for example the extension of reaction time. High concentration of organic and inorganic substances might quench the reactive radical species and could block the active sites on the catalyst surface, remarkably inhibiting generation of free radicals compared to the degradation conducted in the absence of interfering ions [64,74,77,86].

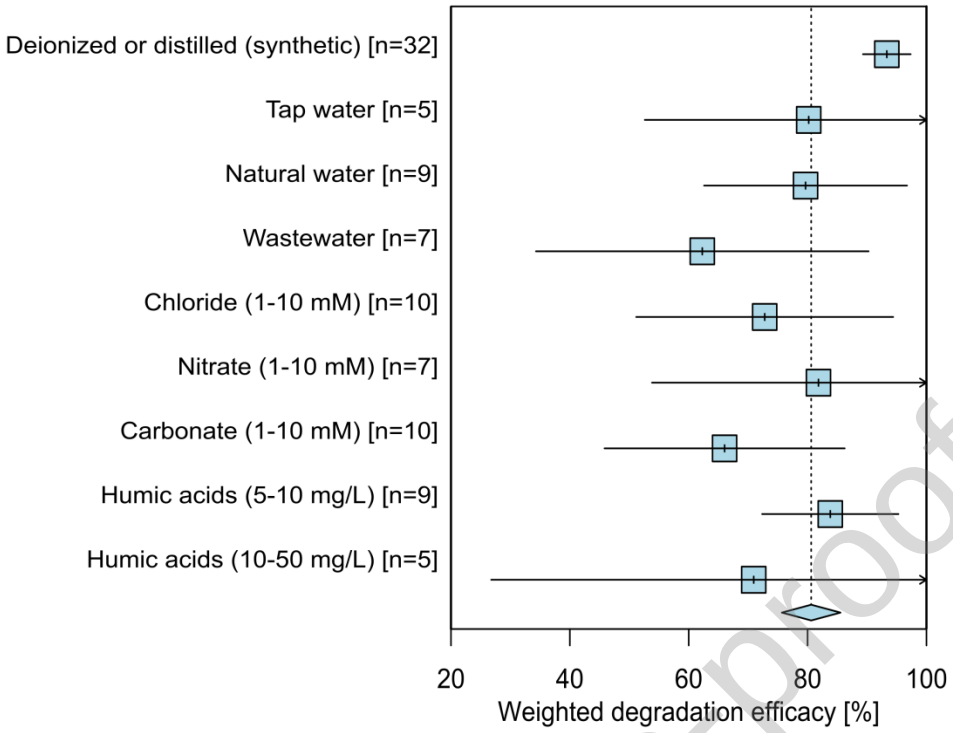

Figure 7. Forest plot of the influence of water matrix characteristics on the weighted degradation efficacy of pesticide/intermediate compounds during the SR-AOPs or PI-AOPs systems, based on the random effects model (CI = 95%) of the average effect size. The vertical black dotted line represents the mean overall degradation efficacy (%) per category. Blue squares indicate the mean degradation efficacy per subgroup. Each effect size is presented as the range between the upper and lower 95% confidence interval. The extend of the blue rectangle represents the confidence interval of the overall degradation efficacy. Group category names are presented on the y-axis black letters. The number of included treatments is given in brackets.

It was revealed that the presence of hydrogen carbonate/carbonate ions also lead to competitive reactions during the investigated heterogeneous AOP, decreasing the process efficacy. HCO_3^- ions (1-10 mM) has inhibitory influence on the degradation of 2,4-D [70,71], atrazine [126] and thiamethoxam [31]. Reactions of $HO^\bullet$ and $SO_4^{\bullet-}$ with HCO_3^- are shown in Eqs. 15-16, resulting with a formation of weaker oxidants such as carbonate and bicarbonate radicals. Reactions of formed $HCO_3^\bullet/CO_3^{\bullet-}$ with electron-rich compounds are significantly lower (2-3 orders of magnitude) than the reaction rate constant with $SO_4^{\bullet-}$ and $HO^\bullet$ [70,126]. Additionally, inhibitory effect can also be a result of the reactions between HCO_3^- and $^1O_2$ (Eq. 17). However, the inhibitory effects of HCO_3^-/CO_3^{2-} on the degradation process by SR-AOPs in natural waters were less pronounced compared to wastewater.

$$HO^\bullet + HCO_3^- \rightarrow CO_3^{\bullet-} + H_2O \quad (15)$$
$$SO_4^{\bullet-} + HCO_3^- \rightarrow SO_4^{2-} + HCO_3^\bullet \quad (16)$$
$$^1O_2 + HCO_3^- \rightarrow CO_3^{\bullet-} + OH^- \quad (17)$$

Water matrix enriched with high concentration of humic acids (up to 50 mg/L HA) has the most pronounced inhibitory effect on the degradation of atrazine and thiamethoxam in ASBC600/US/PMS and FeMn-BC/PS systems, respectively [31,126]. Generally, natural organic matter (NOM) with a high content of aromatic moieties in their structure might scavenge $SO_4^{\bullet-}$ and $HO^\bullet$, with a higher reactions rate of NOM with $HO^\cdot$ (2.23×10^8 $M^{-1}s^{-1}$) than with $SO_4^{\bullet-}$ (6×10^6 $M^{-1}s^{-1}$) indicating the weaker scavenging effect in systems where sulphate radicals are the main radical species [4,127]. On the other hand, HA can adsorb on the catalyst surface competing with oxidant for active sites and further decreasing degradation efficacy [65,128]. However, lower concentration of humic acids (1-10 mg/l) showed negligible inhibition effect on the degradation of 2,4-D [66], thiacloprid [69], 2,4,6-

trichlorophenol [37] and phenol [79].
Additionally, presence of chloride might react with $SO_4^{\bullet-}$ and $HO^{\bullet}$ forming $Cl^{\bullet}$ and $Cl_2^{\bullet-}$ with weaker oxidizing properties, significantly decreasing 2,4-D degradation efficacy by CBC-1/PMS [71], while Jiang et al. (2022) noted that the degradation of atrazine using the S-nZVI@BC/PS system was accelerated in the presence of chloride [67]. Although the degradation process by heterogeneous AOP were affected inevitably by ubiquitous organic matter and inorganic species, high overall WDE within the group indicate the significant potential of investigated processes as a tertiary unit in wastewater treatment plants and for the treatment of refractory pesticides in surface/groundwater.
Kumar et al. (2018) indicated that the existence of HCO_3^- ions and NO_3^- ion can affect the paraquat photodegradion by g-C_3N_4/$Bi_2O_2CO_3$/$CoFe_2O_4$ heterojunction [93]. Due to the lack of data within the selected studies, the influence of water matrix on the photodegradation efficacy was not evaluated in our meta-analysis. Considering the significant water matrix influence on the degradation process and the scarcity of data in the available literature, it is recommended to address this issue in the real application of biochar-based photocatalyst for the pesticide/intermediate removal.

3.8. Current state and future perspectives

The studies evaluated in our paper applied BC-based catalysts in AOP for pesticide and intermediate compound degradation and removal. Available studies provided the preparation and characterization of catalyst, removal kinetics of the target pesticide/intermediate alongside control experiments, quenching tests for the determination of free radical species, and EPR or electron spin resonance analysis. Fundamental research on reaction pathways and degradation mechanisms has only been conducted under laboratory conditions so far. Synergism between BC and the oxidant produces reactive species that boost the performance of AOP compared to sorption alone, reducing the required reaction time and catalyst dose.
However, the degradation intermediates of the target compound, reaction pathways, and the influence of interfering substances are not addressed in all studies evaluated in our meta-analysis. The assessment under real water matrix conditions, testing reusability of catalysts and addressing the method for their separation from treated water should be pivotal for future research. Considering that toxic intermediates can be formed during the degradation process, transformation by-products should be analyzed, accompanying toxicity testing. The use of state-of-the art high-resolution mass spectrometry with a suspect screening methodology approach, which allows a revolutionary ability to track down both known and unknown contaminants and transformation products in real water samples, is highly recommended when treating natural waters and wastewater.
In order to tackle challenges in heterogeneous processes, it is recommended to apply meta-analysis to quantitatively evaluate the impacts of different parameters. However, our analysis showed that a number of individual studies (approx. 23%, section 2.3) did not provide important information that is essential for a detailed and reliable meta-analysis. This mainly includes statistical information such as if and how many replications were conducted and what standard deviation resulted. What could be a way forward would be the establishment of a standard protocol of the publishing journals, according to which a minimum amount of data and information must be reported so that the original study is "ready to use" in meta-analyses. It can also be stated that more original studies are needed, as the application of BC-based catalysts in AOP is a relatively new field of research. The quality and reliability/accuracy of a meta-analysis increases in proportion to the number of studies included. This would help leverage the potential of meta-analysis to gain deeper insights into the efficacy and applicability of such BC-based catalysts. More extensive meta-analysis could then be used to investigate the influence of prevalent intermediates that can be formed and the results of toxicity testing to gain a comprehensive understanding of multiple effects.
Furthermore, the application of the investigated processes in a real water treatment plant requires scaling up the technology to a pilot-stage, considering the techno-economic evaluation of biochar-based catalyst applicability and addressing environmental issues. Further work is advisable to improve the preparation methods for the economically viable and time-efficient production of biochar-based catalysts with sustained stability for large-scale applications. Finally, within the framework of the circular economy concept, the valorization of spent catalysts from AOP, handling and utilization should be considered rather than waste disposal.

4. Conclusions

Our study for the first time comprehensively evaluated the effectiveness of biochar-based catalysts application for (i) PS or PMS and PI activation in SR-AOP and PI-AOP and (ii) in photocatalysis, specifically focusing on the pesticides and its intermediates degradation in water. This meta-analysis systematically summarized the findings of 38 studies (74% studies published during the 2021-2023), with a total of 94 data entries, depending on the observed group and the processes. The following conclusions can be made:

- Depending on the catalyst type, high heterogeneity of the results was observed within the group covering SR-AOP and PI-AOP ($p<0.0243$, $n=31$) while photocatalytic degradation studies did not show significant variability ($p<0.726$, $n=10$). Overall WDE of pesticides/intermediate compounds was similar for both groups of processes (91.8-92.4% WDE). The most effective pesticides/intermediate compounds degradation enabled systems including the metal and non-metal co-doped biochar catalyst (e.g. FeS@BC/PMS, PCoFe@BC_5/PMS, S-nZVI@BC/PS) and multicomponent heterojunction (e.g. g-C_3N_4/$Bi_2O_2CO_3$/$CoFe_2O_4$, BC/CdS-Fe_3O_4) exposed to simulated solar light (94.7-98.8% WDE).
- Properties of the applied oxidant, PS, PMS and PI did not exhibit significant influence on the WDE ($p=0.1979$). Studies investigated the application of PMS showed slightly higher variability of the results than articles studied PS activation.
- pH has a strong influence on the pesticides/intermediate compounds degradation using heterogeneous SR-AOP and PI-AOP ($p=0.0207$, $n=95$). Degradation efficacy for both groups of processes was the most effective within pH 5-8 range and significantly drops with increasing of pH (≥9).
- WDE achieved by heterogeneous SR-AOP and PI-AOP was strongly affected by the chemical properties of pesticides and intermediate compounds. Organochlorine pesticides and intermediates characterized by mediate level of hydrophobicity ($2 < \log Kow < 4$) was the most susceptible to degradation.
- Development of photocatalyst with biochar support enables effective absorption of sunlight, particularly visible light, resulting in high degradation efficacy.
- Efficacy of SR-AOP or PI-AOP systems significantly decreased in the presence of interfering ions compared to the degradation in deionized/distilled water. Wastewater expressed the most pronounced influence on the WDE followed by the water containing hydrogencarbonate (1-10 mM) and humic acids (10-50 mg/l HA).

Biochar as catalytic support provides remarkable approach toward challenges in the removal of refractory pollutants in AOP water treatment compared to the adsorption and photolysis. Investigated systems have a significant potential to boost not only the performance of tertiary units in wastewater treatment plants but also the treatment of surface and groundwater.

Acknowledgements Funded by the European Union. Grant agreement No. 101059546.

Author's contributions

BG and JMJ contributed to the study conception and design, writing-reviewing, editing and supervising. JMJ, JN, TS, JA conducted the literature search and data collection. BG and AG performed meta-analysis and discussion. JMJ, BG, AG, SM prepared manuscript draft. All the co-authors commented on the manuscript and approved the final manuscript.

Funding

Funded by the European Union. Views and opinions expressed are however those of the author(s) only and do not necessarily reflect those of the European Union or European Research Executive Agency (REA). Neither the European Union nor the granting authority can be held responsible for them. Grant agreement No. 101059546.

Data availability

Raw data are available at https://zenodo.org/records/10548741

Declarations

Competing interests: The authors do not have any competing interests.

References

[1] H. Liu, J. Long, K. Zhang, M. Li, D. Zhao, D. Song, W. Zhang, Agricultural biomass/waste-based materials could be a potential adsorption-type remediation contributor to environmental pollution induced by pesticides-A critical review, Sci. Total. Environ. 946 (2024) 174180. https://doi.org/10.1016/j.scitotenv.2024.174180
[2] W. Zhou, M. Li, V. Achal, A comprehensive review on environmental and human health impacts of chemical pesticide usage, Emerg. Contam. 11 (2025) 100410. https://doi.org/10.1016/j.emcon.2024.100410
[3] L. Rizzo, W. Gernjak, P. Krzeminski, S. Malato, C.S. McArdell, J.A. Sanchez Perez, H. Schaar, D. Fatta-Kassinos, Best available technologies and treatment trains to address current challenges in urban wastewater reuse for irrigation of crops in EU countries, Sci. Total. Environ. 710 (2020) 136321. https://doi.org/10.1016/j.scitotenv.2019.136312
[4] J. Molnar Jazić, T. Đurkić, B. Bašić, M. Watson, T. Apostolović, J. Agbaba, Degradation of a chloroacetanilide herbicide in natural waters using UV activated hydrogen peroxide, persulfate and peroxymonosulfate processes, Environ. Sci. Water Res. Technol. 6 (2020) 2800 - 2815. https://doi.org/10.1039/D0EW00358A
[5] I.A. Saleh, N. Zouari, M.A. Al-Ghouti, Removal of pesticides from water and wastewater: Chemical, physical and biological treatment approaches, Environ. Technol. Innov. 19 (2020) 101026. https://doi.org/10.1016/j.eti.2020.101026
[6] X. Li, B. Jie, H. Lin, Z. Deng, J. Qian, Y. Yang, X. Zhang, Application of sulfate radicals-based advanced oxidation technology in degradation of trace organic contaminants (TrOCs): Recent advances and prospects, J. Environ. Manage. 308 (2022) 114664. https://doi.org/10.1016/j.jenvman.2022.114664
[7] J. Gao, T. Qin, S. Wacławek, X. Duan, Y. Huang, H. Liu, D.D. Dionysiou, The application of advanced oxidation processes (AOPs) to treat unconventional water for fit-for-purpose reuse, Curr. Opin. Chem. Eng. 42 (2023) 100974. https://doi.org/10.1016/j.coche.2023.100974
[8] D. Yalin, H.A. Craddock, S. Assouline, E.B. Mordechay, A. Ben-Gal, N. Bernstein, R.M. Chaudhry, B. Chefetz, D. Fatta-Kassinos, B.M. Gawlik, K.A. Hamilton, L. Khalifa, I. Kisekka, I. Klapp, H. Korach-Rechtman, D. Kurtzman, G.J. Levy, R. Maffettone, S. Malato, C.M. Manaia, K. Manoli, O.F. Moshe, A. Rimelman, L. Rizzo, D.L. Sedlak, M. Shnit-Orland, E. Shtull-Trauring, J. Tarchitzky, V. Welch-White, C. Williams, J. McLain, E. Cytryn, Mitigating risks and maximizing sustainability of treated wastewater reuse for irrigation, Water Res. X 21 (2023) 100203. https://doi.org/10.1016/j.wroa.2023.100203
[9] Z.U. Khan, N.S. Gul, S. Sabahat, J, Sun, K. Tahir, N.S. Shah, N. Muhammad, A. Rahim, M. Imran, J. Iqbal, T.M. Khan, S. Khasim, U. Farooq, J. Wu, Removal of organic pollutants through hydroxyl radical-based advanced oxidation processes, Ecotoxicol. Environ. Saf. 267 (2023) 115564. https://doi.org/10.1016/j.ecoenv.2023.115564
[10] S. Giannakis, K-Y.A. Lin, F. Ghanbari, A review of the recent advances on the treatment of industrial wastewaters by Sulfate Radical-based Advanced Oxidation Processes (SR-AOPs), Chem. Eng. J. 406 (2020) 127083. https://doi.org/10.1016/j.cej.2020.127083
[11] Q. Yang, Q. Ma, F. Chen, F. Yao, J. Sun, S. Wang, K. Yi, L. Hou, X. Li, D. Wang, Recent advances in photo-activated sulfate radical-advanced oxidation process (SR-AOP) for refractory organic pollutants removal in water. Chem Eng. J. 378 (2019) 122149. https://doi.org/10.1016/j.cej.2019.122149
[12] J. Scaria, P.V. Nidheesh, Comparison of hydroxyl-radical-based advanced oxidation processes with sulfate radical-based advanced oxidation processes, Curr. Opin. Chem. Eng. 36 (2022) 100830. https://doi.org/10.1016/j.coche.2022.100830
[13] J. Dai, Z. Wang, K. Chen, D. Ding, S. Yang, T. Cai, Applying a novel advanced oxidation process of biochar activated periodate for the efficient degradation of bisphenol A: Two nonradical pathways, Chem. Eng. J. 453 (2023), 139889. https://doi.org/10.1016/j.cej.2022.139889
[14] H. Yang, C-G. Lee, J. Lee, Utilizing animal manure-derived biochar in catalytic advanced oxidation processes: A review, J. Water Process Eng. 56 (2023) 104545. https://doi.org/10.1016/j.jwpe.2023.104545

[15] U. Ushani, X. Lu, J. Wang, Z. Zhang, J. Dai, Y. Tan, S. Wang, W. Li, C. Niu, T. Cai, N. Wang, G. Zhen, Sulfate radicals-based advanced oxidation technology in various environmental remediation: A state-of-the–art review, Chem. Eng. J. 402 (2023) 126232. https://doi.org/10.1016/j.cej.2020.126232
[16] B. Yu, Y. Man, P. Wang, C. Wu, J. Xie, W. Wang, H. Jiang, L. Zhang, Y. Zhang, L. Mao, L. Zhu, Y. Zheng, X. Liu, Catalytic degradation of dimethomorph by nitrogen-doped rice husk biochar, Ecotoxicol. Environ. Saf. 257 (2023) 114908. https://doi.org/10.1016/j.ecoenv.2023.114908
[17] X. Zhang, T. Bhattacharya, C. Wang, A. Kumar, P.V. Nidheesh, Straw-derived biochar for the removal of antibiotics from water: Adsorption and degradation mechanisms, recent advancements and challenges, Environ. Res. 237 (2023) 116998. https://doi.org/10.1016/j.envres.2023.116998
[18] X. Chen, L. Fu, Y. Yu, C. Wu, M. Li, X. Jin, J. Yang, P. Wang, Y. Chen, Recent Development in Sludge Biochar-Based Catalysts for Advanced Oxidation Processes of Wastewater, Catal. 11 (2021) 1275. https://doi.org/10.3390/catal11111275
[19] A. Dutta Gupta, H. Singh, S. Varjani, M. Kumar Awasthi, B. Shekhar Giri, A. Pandey, A critical review on biochar-based catalysts for the abatement of toxic pollutants from water via advanced oxidation processes (AOPs), Sci. Total. Environ. 849 (2022) 157831. http://dx.doi.org/10.1016/j.scitotenv.2022.157831
[20] B. Glaser, M. Guenther, H. Maennicke, T. Bromm, Microwave-assisted combustion to produce benzene polycarboxylic acids as molecular markers for biochar identification and quantification, Biochar 3 (2021) 407 – 418. https://doi.org/10.1007/s42773-021-00124-z
[21] S. Jesus Duarte, A. Hubach, B. Glaser, Soil water balance and wettability methods in soil treated with biochar and/or compost, Carbon Res. 1 (2022) 31. https://doi.org/10.1007/s44246-022-00032-2
[22] C. Wang, R. Huang, R. Sun, J. Yang, M. Sillanpää, A review on persulfates activation by functional biochar for organic contaminants removal: Synthesis, characterizations, radical determination, and mechanism, J. Environ. Chem. Eng. 9 (2021) 106267. https://doi.org/10.1016/j.jece.2021.106267
[23] F. Li, F. Duan, W. Jia, X. Gui, Biochar-activated persulfate for organic contaminants removal: Efficiency, mechanisms and influencing factors, Ecotoxicol. Environ. Saf. 198 (2020) 110653. https://doi.org/10.1016/j.ecoenv.2020.110653
[24] J. Lu, Q. Lu, L. Di, Y. Zhou, Y. Zhou, Iron-based biochar as efficient persulfate activation catalyst for emerging pollutants removal: A review, Chin. Chem. Lett. 31 (11) (2023) 108357. https://doi.org/10.1016/j.cclet.2023.108357
[25] T. Jiang, B. Wang, B. Gao, N. Cheng, Q. Feng, M. Chen, S. Wang, Degradation of organic pollutants from water by biochar-assisted advanced oxidation processes: Mechanisms and applications, J. Hazard. Mater. 442 (2023) 130075. https://doi.org/10.1016/j.jhazmat.2022.130075
[26] C. Wang, X. Lin, X. Zhang, P.L. Show, Research advances on production and application of algal biochar in environmental remediation, Environ. Pollut. 348 (2024) 123860. https://doi.org/10.1016/j.envpol.2024.123860
[27] H. Nan, R. Huang, X. Zhang, C. Wang, How does ball-milling elevate biochar as a value-added peroxydisulfate activator for antibiotics removal? Ind. Crop. Prod. 214 (2024) 118569. https://doi.org/10.1016/j.indcrop.2024.118569
[28] C. Wang, R. Huang, R. Sun, J. Yang, M. Sillanpää, A review on persulfates activation by functional biochar for organic contaminants removal: Synthesis, characterizations, radical determination, and mechanism, J. Environ. Chem. Eng. 9 (2021) 106267. https://doi.org/10.1016/j.jece.2021.106267
[29] H. Chen, Y. Gao, J. Li, Z. Fang, N. Bolan, A. Bhatnagar, B. Gao, D. Hou, S. Wang, H. Song, X. Yang, S.M. Shaheen, J. Meng, W. Chen, J. Rinklebe, H. Wang, Engineered biochar for environmental decontamination in aquatic and soil systems: a review, Carbon Res. 1 (2022) 4. https://doi.org/10.1007/s44246-022-00005-5
[30] X. Yang, Z. Guo, X. Chen, S. Xi, K. Cui, J. Li, D. Dong, F. Wu, Z. Wu, Efficient degradation of thiamethoxam pesticide in water by iron and manganese oxide composite biochar activated persulfate, Chem. Eng. J. 473 (2023) 145051. https://doi.org/10.1016/j.cej.2023.145051
[31] Y. Yang, Z. Kang, G. Xu, J. Wang, Y. Yu, Degradation of bensulfuron methyl by nitrogen/boron codoped biochar activated peroxydisulfate at lower temperature, J. Clean Prod. 402 (2023) 136816. https://doi.org/10.1016/j.jclepro.2023.136816

[32] J. Deng, Y. Zeng, E. Almatrafi, Y. Liang, Z. Wang, Z. Wang, B. Song, Y. Shang, W. Wang, C. Zhou, G. Zeng, Advances of carbon nitride based atomically dispersed catalysts from single-atom to dual-atom in advanced oxidation process applications, Coord. Chem. Rev. 505 (2024) 215693. https://doi.org/10.1016/j.ccr.2024.215693
[33] T. Zhou, J. Deng, Y. Zeng, X. Liu, B. Song, S. Ye, M. Li, Y. Yang, Z. Wang, C. Zhou, Biochar Meets Single-Atom: A Catalyst for Efficient Utilization in Environmental Protection Applications and Energy Conversion, Small. 10 (2024) 2404254. https://doi.org/10.1002/smll.202404254
[34] Z. Jiang, J. Li, D. Jiang, Y. Gao, Y. Chen, W. Wang, B. Cao, Y. Tao, L. Wang, Y. Zhang, Removal of atrazine by biochar-supported zero-valent iron catalyzed persulfate oxidation: Reactivity, radical production and transformation pathway, Environ. Res. 184 (2020) 109260. https://doi.org/10.1016/j.envres.2020.109260
[35] Y. Chen, D. Ouyang, W. Zhang, J. Yan, L. Qian, L. Han, M. Chen, Degradation of benzene derivatives in the CuMgFe-LDO/persulfate system: The role of the interaction between the catalyst and target pollutants, J. Environ. Sci. 90 (2020) 87-97. https://doi.org/10.1016/j.jes.2019.11.014
[36] R. Li, Y. Wen, M. Liu, L. Su, Y. Wang, S. Li, M. Zhong, Z. Zhou, N. Zhou, Simultaneous removal of organic inorganic composite contaminants by in situ double modified biochar: Performance and mechanisms, J. Taiwan Inst. Chem. Eng. 139 (2022) 104523. https://doi.org/10.1016/j.jtice.2022.104523
[37] H. Li, S. Li, L. Jin, Z. Lu, M. Xiang, C. Wang, W. Wang, J. Zhang, C. Li, H. Xie, Activation of peroxymonosulfate by magnetic Fe_3S_4/biochar composites for the efficient degradation of 2,4,6-trichlorophenol: Synergistic effect and mechanism, J. Environ. Chem. Eng. 10 (2022) 107085. https://doi.org/10.1016/j.jece.2021.107085
[38] Issaka, E., Fapohunda, F.O., Amu-Darko, J.N.O., Yeboah, L., Yakubu, S., Varjani, S., Ali, N., Bilal, M., 2022. Biochar-based composites for remediation of polluted wastewater and soil environments: Challenges and prospects. Chemosphere 297, 134163. https://doi.org/10.1016/j.chemosphere.2022.134163
[39] F. Abbaci, A. Nait-Merzoug, O. Guellati, A. Harat, J. El Haskouri, J. Delhalle, Z. Mekhalif, M. Guerioune, Bio/KOH ratio effect on activated biochar and their dye based wastewater depollution, J. Anal. Appl. Pyrolysis 162 (2022) 105452. https://doi.org/10.1016/j.jaap.2022.105452
[40] D. Kalampaliki, G.D.T.M. Jayasinghe, E. Avramiotis, I.D. Manariotis, D. Venieri, S.G. Poulopoulos, J. Szpunar, J. Vakros, D. Mantzavinos, Application of a KOH-activated biochar for the activation of persulfate and the degradation of sulfamethoxazole, Chem. Eng. Res. Des. 194 (2023) 306 - 317. https://doi.org/10.1016/j.cherd.2023.04.056
[41] Z. Wei, F.A. Villamena, L.K. Weavers, Kinetics and mechanism of ultrasonic activation of persulfate: an in situ EPR spin trapping study, Environ. Sci. Technol. 51:6 (2017) 3410 - 3417. https://doi.org/10.1021/acs.est.6b05392
[42] T. Zhang, S. Wu, N. Li, G. Chen, L. Hou, Applications of vacancy defect engineering in persulfate activation: Performance and internal mechanism, J. Hazard. Mater. 449 (2023) 130971. https://doi.org/10.1016/j.jhazmat.2023.130971
[43] Y. Zhang, B. Zhou, H. Chen, R. Yuan, Heterogeneous photocatalytic oxidation for the removal of organophosphorus pollutants from aqueous solutions: A review, Sci. Total. Environ. 856 (2023) 159048. http://dx.doi.org/10.1016/j.scitotenv.2022.159048
[44] Y-Y. Ahn, E.T. Yun, Heterogeneous metals and metal-free carbon materials for oxidative degradation through persulfate activation: A review of heterogeneous catalytic activation of persulfate related to oxidation mechanism, Korean J. Chem. Eng. 36 (11) (2022) 1767 - 1779. https://doi.org/10.1007/s11814-019-0398-4
[45] S. Farahbakhsh, R. Parvari, A. Zare, H. Mahdizadeh, V. Faizi, A. Saljooqi, Preparation of biochar based on grapefruit peel and magnetite decorated with cadmium sulfide nanoparticles for photocatalytic degradation of chlorpyrifos, Diam. Relat. Mater. 126 (2022) 109130. https://doi.org/10.1016/j.diamond.2022.109130
[46] B. Başer, B. Yousaf, U. Yetis, Q. Abbas, E.E. Kwon, S. Wang, N.S. Bolan, J. Rinklebe, Formation of nitrogen functionalities in biochar materials and their role in the mitigation of hazardous emerging organic pollutants from wastewater, J. Hazard. Mater. 416 (2021) 126131. https://doi.org/10.1016/j.jhazmat.2021.126131
[47] A. Ahmad, M. Priyadarshini, S. Yadav, M.M. Ghangrekar, R.Y. Surampalli, The potential of

biochar-based catalysts in advanced treatment technologies for efficacious removal of persistent organic pollutants from wastewater: A review, Chem. Eng. Res. Des. 187 (2022) 470 - 496. https://doi.org/10.1016/j.cherd.2022.09.024
[48] Y. Cao, X. Yuan, Y. Zhao, H. Wang, In-situ soil remediation via heterogeneous iron-based catalysts activated persulfate process: A review, Chem. Eng. J. 431 (2022) 133833. https://doi.org/10.1016/j.cej.2021.133833
[49] W. Liu, Y. Lu, Y. Dong, Q. Jin, H. Lin, A critical review on reliability of quenching experiment in advanced oxidation processes, Chem. Eng. J. 466 (2023) 143161. https://doi.org/10.1016/j.cej.2023.143161
[50] X. Chen, B. Wu, W. Yang, G. Zhao, J. Han, C. Huang, B. Sun, A. Wang, Z. Li, Biochar as a multifunctional material facilitate the organohalide remediation: A state-of-the-art review, Chem. Eng. J. 460 (2023) 141700. https://doi.org/10.1016/j.cej.2023.141700
[51] B. Cui, T. Tian, L. Duan, H. Rong, Z. Chen, S. Luo, D. Guo, R. Naidu, Towards advanced removal of organics in persulfate solution by heterogeneous iron-based catalyst: A review, J. Environ. Sci. 146 (2024) 163-175. https://doi.org/10.1016/j.jes.2023.06.035
[52] Faheem, J. Du, S.H. Kim, M.A. Hassan, S. Irshad, J. Bao, Application of biochar in advanced oxidation processes: supportive, adsorptive, and catalytic role, Environ. Sci. Pollut. R. 27 (2020) 37286-37312. https://doi.org/10.1007/s11356-020-07612-y
[53] M. Faisal Gasim, J.-W. Lim, S.-C. Low, K.-Y. Andrew Lin, W.-D. Oh, Can biochar and hydrochar be used as sustainable catalyst for persulfate activation?, Chemosphere 287 (2022) 132458. https://doi.org/10.1016/j.chemosphere.2021.132458
[54] W. Huang, S. Xiao, H. Zhong, M. Yan, X. Yang, Activation of persulfates by carbonaceous materials: A review, Chem.Eng. J. 418 (2021) 129297. https://doi.org/10.1016/j.cej.2021.129297
[55] J. Ji, X. Yuan, Y. Zhao, L. Jiang, H. Wang, Mechanistic insights of removing pollutant in adsorption and advanced oxidation processes by sludge biochar, J. Hazard. Mater. 430 (2022) 128375. https://doi.org/10.1016/j.jhazmat.2022.128375
[56] P.V. Nidheesha, A. Gopinatha, N. Ranjitha, A.P. Akrea, V. Sreedharanb, M.S. Kumar, Potential role of biochar in advanced oxidation processes: A sustainable approach, Chem.Eng. J. 405 (2021) 126582. https://doi.org/10.1016/j.cej.2020.126582
[57] Q. Song, F. Kong, B.-F. Liu, X. Song, H.-Y. Ren, Biochar-based composites for removing chlorinated organic pollutants: Applications, mechanisms, and perspectives, Environ Sci Ecotech. 21 (2024) 100420. https://doi.org/10.1016/j.ese.2024.100420
[58] Z. Guo, J. Li, Z. Zhang, Meta-analysis for systematic review of global micro/nano-plastics contamination versus various freshwater microalgae: Toxicological effect patterns, taxon-specific response, and potential eco-risks, Water Res. 258 (2024) 121706. https://doi.org/10.1016/j.watres.2024.121706
[59] S.A. Khan, M. Jain, K.K. Pant, Z.M. Ziora, M.A.T. Blaskovich, Photocatalytic degradation of parabens: A comprehensive meta-analysis investigating the environmental remediation potential of emerging pollutant, Sci. Total Environ. 920 (2024) 171020. https://doi.org/10.1016/j.scitotenv.2024.171020
[60] L. Ricolfi, M.D. Taylor, Y. Yang, M. Lagisz, S. Nakagawa, Maternal transfer of per- and polyfluoroalkyl substances (PFAS) in wild birds: A systematic review and meta-analysis, Chemosphere 361 (2024) 142346. https://doi.org/10.1016/j.chemosphere.2024.142346
[61] M. Malakootian, A. Shahesmaeili, M. Faraji, H. Amiri, S.S. Martinez, Advanced oxidation processes for the removal of organophosphorus pesticides in aqueous matrices: A systematic review and meta-analysis, Process Saf. Environ. Prot. 134 (2020) 292-307. https://doi.org/10.1016/j.psep.2019.12.004
[62] M. Yeganeh, E. Charkhloo, H.R. Sobhi, A. Esrafili, M. Gholami, Photocatalytic processes associated with degradation of pesticides in aqueous solutions: Systematic review and meta-analysis, Chem. Eng. J. 428 (2022) 130081. https://doi.org/10.1016/j.cej.2021.130081
[63] M. Moazeni, M.R. Maracy, R. Ghazavi, J. Bedia, K-Y.A. Lin, A. Ebrahimi, Removal of triclosan from aqueous matrixes: A systematic review with detailed meta-analysis, J. Mol. Liq. 376 (2023) 121450. https://doi.org/10.1016/j.molliq.2023.121450
[64] E.A. El-Bestawy, M. Gaber, H. Shokry, M. Samy, Effective degradation of atrazine by spinach-derived biochar via persulfate activation system: Process optimization, mechanism, degradation

pathway and application in real wastewater, Environ. Res. 229 (2023) 115987. https://doi.org /10.1016/j.envres.2023.115987
[65] W. Jia, H. Wang, Q. Wu, L. Sun, Q. Si, Q. Zhao, Y. Wu, N. Ren, W. Guo, Insight into Chinese medicine residue biochar combined with ultrasound for persulfate activation in atrazine degradation: Acanthopanax senticosus precursors, synergistic effects and toxicity assessment. Sci. Total Environ. 880 (2023) 163054. http://dx.doi.org/10.1016/j.scitotenv.2023.163054
[66] X. Liang, Y. Zhao, J. Liu, Z. Yang, Q. Yang, Highly efficient activation of peroxymonosulfate by cobalt ferrite anchored in P-doped activated carbon for degradation of 2,4-D:Adsorption and electron transfer mechanism, J. Colloid Interface Sci. 642 (2023) 757 - 770. https://doi.org /10.1016/j.jcis.2023.03.181
[67] Q. Jiang, S. Jiang, H. Li, R. Zhang, Z. Jiang, Y. Zhang, A stable biochar supported S-nZVI to activate persulfate for effective dichlorination of atrazine, Chem. Eng. J. 431 (2022) 133937. https://doi.org/10.1016/j.cej.2021.133937
[68] P. Huang, P. Zhang, C. Wang, J. Tang, H. Sun, Enhancement of persulfate activation by Fe-biochar composites: Synergism of Fe and N-doped biochar, Appl. Catal. B-Environ. 303 (2022) 120926. https://doi.org/10.1016/j.apcatb.2021.120926
[69] L. He, Y. Shi, Y. Chen, S. Shen, J. Xue, Y. Ma, L. Zheng, L. Wu, Z. Zhang, L. Yang, Iron-manganese oxide loaded sludge biochar as a novel periodate activator for thiacloprid efficient degradation over a wide pH range, Sep. Purif. Technol. 288 (2022) 120703. https://doi.org/ 10.1016/j.seppur.2022.120703
[70] Q. Hong, C. Liu, Z. Wang, R. Li, X. Liang, Y. Wang, Y. Zhang, Z. Song, Z. Xiao, T. Cui, B. Heng, B. Xu, F. Qi, A. Ikhlaq, Electron transfer enhancing Fe(II)/Fe(III) cycle by sulfur and biochar in magnetic FeS@biochar to active peroxymonosulfate for 2,4-dichlorophenoxyacetic acid degradation, Chem. Eng. J. 417 (2021) 129238. https://doi.org/10.1016/j.cej.2021.129238
[71] X. Liang, Y. Zhao, N. Guo, Q. Yang, Heterogeneous activation of peroxymonosulfate by Co_3O_4 loaded biochar for efficient degradation of 2,4-dichlorophenoxyacetic acid, Colloids Surf A: Physicochem. Eng. Asp. 627 (2021) 127152. https://doi.org/10.1016/j.colsurfa.2021.127152
[72] Y. Zhang, Q. Jiang, S. Jiang, H. Li, R. Zhang, J. Qu, S. Zhang, W. Han, One-step synthesis of biochar supported nZVI composites for highly efficient activating persulfate to oxidatively degrade atrazine, Chem. Eng. J. 420 (2021) 129868. https://doi.org/10.1016/j.cej.2021.129868
[73] W. Hayat, Y. Zhang, I. Hussain, S. Huang, X. Du, Comparison of radical and non-radical activated persulfate systems for the degradation of imidacloprid in water, Ecotoxicol. Environ. Saf. 188 (2020) 109891. https://doi.org/10.1016/j.ecoenv.2019.109891
[74] S. Wang, J. Wang, Activation of peroxymonosulfate by sludge-derived biochar for the degradation of triclosan in water and wastewater, Chem. Eng. J. 356 (2019) 350 - 358. https://doi.org/10.1016/j.cej.2018.09.062
[75] C. Liu, L. Chen, D. Ding, T. Cai, From rice straw to magnetically recoverable nitrogen doped biochar: Efficient activation of peroxymonosulfate for the degradation of metolachlor, Appl. Catal. B Environ. 254 (2019) 312 - 320. https://doi.org/10.1016/j.apcatb.2019.05.014
[76] K. Zhang, D. Huang, Y. Zhang, N. El Houda Bouroubi, P. Chen, N. Ganbold, P. He, J. Liu, Y. Fang, M. Gan, J. Zhu, B. Yang, Natural mineral-derived Fe/Mn-BC as efficient peroxydisulfate activator for 2,4-dichlorophenol removal from wastewater: Performance and sustainable catalytic mechanism, J. Environ. Manage. 335 (2023) 117540. https://doi.org/10.1016/j.jenvman.2023.117540
[77] S. Zhong, J. Pan, K. Tian, J. Qin, T. Qing, J. Zhang, Efficient degradation of p-chlorophenol by N,S-codoped biochar activated perxymonosulfate, Process Saf. Environ. Prot. 169 (2023) 437 - 446. https://doi.org/10.1016/j.psep.2022.10.081
[78] S. Tong, D. Chen, X. Jiang, Z. Xu, X. Liu, J. Shen, Persulfate activation by Fe_3O_4-doped biochar synthesized from Fenton sludge and sewage sludge for enhanced 1-H-1,2,4-triazole degradation, Chem. Eng. J. 461 (2023) 142075. https://doi.org/10.1016/j.cej.2023.142075
[79] K. Miserli, D. Kogola, I. Paraschoudi, I. Konstantinou, Activation of persulfate by biochar for the degradation of phenolic compounds in aqueous systems, Chem. Eng. J. Adv. 9 (2022) 100201. https://doi.org/10.1016/j.ceja.2021.100201
[80] Z. Zhi, D. Wu, F. Meng, Y. Yin, B. Song, Y. Zhao, M. Song, Facile synthesis of $CoFe_2O_4$@BC activated peroxymonosulfate for p-nitrochlorobenzene degradation: Matrix effect and toxicity evaluation, Sci. Total Environ. 828 (2022) 154275. http://dx.doi.org/10.1016/j.scitotenv.2022.154275

[81] X. Wang, R. Deng, W. Shen, J. Huang, Q. Li, Y. Zhao, J. Wan, Y. Zhou, T. Long, S. Zhang, Rapid Degradation of Nitrochlorobenzene by Activated Persulfate Oxidation With Biochar Supported Nanoscaled Zero Valent Iron, Front. Chem. 10:9 (2021) 615694. https://doi.org/10.3389/fchem.2021.615694
[82] B. Wang, C. Zhu, D. Ai, Z. Fan, Activation of persulfate by green nano-zero-valent iron-loaded biochar for the removal of p-nitrophenol: Performance, mechanism and variables effects, J. Hazard. Mater. 417 (2021) 126106. https://doi.org/10.1016/j.jhazmat.2021.126106
[83] L. Yang, Y. Chen, D. Ouyang, J. Yan, L. Qian, L. Han, M. Chen, J. Li, M. Gud, Mechanistic insights into adsorptive and oxidative removal of monochlorobenzene in biochar-supported nanoscale zero-valent iron/persulfate system, Chem. Eng. J. 400 (2020) 125811. https://doi.org/10.1016/j.cej.2020.125811
[84] H. Zhou, X. Zhu, B. Chen, Magnetic biochar supported α-MnO_2 nanorod for adsorption enhanced degradation of 4-chlorophenol via activation of peroxydisulfate, Sci. Total Environ. 724 (2020) 138278. https://doi.org/10.1016/j.scitotenv.2020.138278
[85] S. Chenfei, L. Yumeng, F. Haiyao, J. Shumin, X. Ruijie, L. Gang, W. Guoxiang, Removal of p-Nitrophenol Using Persulfate Activated by Biochars Prepared from Different Biomass Materials, Chem. Res. Chin. Univ. 34(1) (2018) 39 - 43. https://doi.org/10.1007/s40242-017-7245-0
[86] J. Wang, Z. Liao, J. Ifthikar, L. Shi, Y. Du, J. Zhu, S. Xi, Z. Chen, Z. Chen, Treatment of refractory contaminants by sludge-derived biochar/persulfate system via both adsorption and advanced oxidation process, Chemosphere 185 (2017) 754 - 763. http://dx.doi.org/10.1016/j.chemosphere.2017.07.084
[87] C. Zhang, Z. Yu, X. Wang, B. Wang, Enhanced visible light assisted peroxymonosulfate process by biochar in-situ enriched with γ-Fe_2O_3 for p-chlorophenol degradation: performance, mechanism and DFT calculation, J. Hazard. Mater. 445 (2023) 130593. https://doi.org/10.1016/j.jhazmat.2022.130593
[88] M. Zahedifar, N. Seyedi, Bare 3D-TiO_2/magnetic biochar dots (3D-TiO_2/BCDs MNPs): Highly efficient recyclable photocatalyst for diazinon degradation under sunlight irradiation, Phys. E Low-Dimens. Syst. Nanostructures 139 (2022) 115151. https://doi.org/10.1016/j.physe.2022.115151
[89] X. An, H. Wang, C. Dong, P. Jiang, Z. Wu, B. Yu, Core-shell P-laden biochar/ZnO/g-C_3N_4 composite for enhanced photocatalytic degradation of atrazine and improved P slow-release performance, J. Colloid Interface Sci. 608 (2022) 2539 - 2548. https://doi.org/10.1016/j.jcis.2021.10.166
[90] X. An, Y. Chen, M. Ao, Y. Jin, L. Zhan, B. Yu, Z. Wu, P. Jiang, Sequential photocatalytic degradation of organophosphorus pesticides and recovery of orthophosphate by biochar/α-Fe_2O_3/MgO composite: A new enhanced strategy for reducing the impacts of organophosphorus from wastewater, Chem. Eng. J. 435 (2022) 135087. https://doi.org/10.1016/j.cej.2022.135087
[91] K. Serelis, N. Mantzos, D. Meintani, I. Konstantinou, The effect of biochar, hydrochar particles and dissolved organic matter on the photodegradation of metribuzin herbicide in aquatic media, J. Environ. Chem. Eng. 9 (2021) 105027. https://doi.org/10.1016/j.jece.2021.105027
[92] P.T. Le, D.N. Le, T.H. Nguyen, H.T. Bui, L.A. Pham, L.L. Nguyen, Q.S. Nguyen, T.P. Nguyen, T.H. Dang, T.T. Duong, M. Herrmann, S. Ouillon, T.P.Q. Le, D.L. Vo, H. Mai, T.M.T. Dinh, On the Degradation of Glyphosate by Photocatalysis Using TiO_2/Biochar Composite Obtained from the Pyrolysis of Rice Husk, Water 13 (2021) 3326. https://doi.org/10.3390/w13233326
[93] A. Kumar, A. Kumar, G. Sharma, A.H. Al-Muhtaseb, M. Naushad, A.A. Ghfar, C. Guo, F.J. Stadler, Biochar-templated g-C_3N_4/$Bi_2O_2CO_3$/$CoFe_2O_4$ nano-assembly for visible and solar assisted photo-degradation of paraquat, nitrophenol reduction and CO_2 conversion, Chem. Eng. J. 339 (2018) 393 - 410. https://doi.org/10.1016/j.cej.2018.01.105
[94] M.V. Pinna, S. Baronti, F. Miglietta, A. Pusino, Photooxidation of foramsulfuron: Effects of char substances, J. Photochem. Photobiol. A Chem. 326 (2016) 16 - 20. http://dx.doi.org/10.1016/j.jphotochem.2016.04.014
[95] T.A. Furukawa, C. Barbui, A. Cipriani, P. Brambilla, Watanabe N. Imputing missing standard deviations in meta-analyses can provide accurate results, J. Clin. Epidemiol. 59(1) (2006) 7 - 10. https://doi.org/10.1016/j.jclinepi.2005.06.006
[96] W. Viechtbauer, Bias and Efficiency of Meta-Analytic Variance Estimators in the Random-Effects Model, J. Educ. Behav. Stat. 30 (3) (2005) 261 - 293. https://doi.org/

10.3102/10769986030003261
[96] M. Harrer, P. Cuijpers, T.A. Furukawa, D.D. Ebert, Doing Meta-Analysis with R: A Hands-On Guide. Boca Raton, FL and London: Chapman & Hall/CRC Press (2021).
[97] R. Core Team, R: A language and environment for statistical computing. R Foundation for Statistical Computing, Vienna, Austria, (2021). URL https://www.R-project.org/.
[98] S. Balduzzi, G. Rücker, G. Schwarzer, How to perform a meta-analysis with R: A practical tutorial. Evid.-Based Ment, Health 22 (2019) 153 - 160. https://doi.org/10.1136/ebmental-2019-300117
[99] X. Duan, Z. Ao, D. Li, H. Sun, L. Zhou, A. Suvorova, M. Saunders, G. Wang, S. Wang, Surface-tailored nanodiamonds as excellent metal-free catalysts for organic oxidation, Carbon 103 (2016) 404 - 411. http://dx.doi.org/10.1016/j.carbon.2016.03.034
[100] A. Javanmard, W.M.A.B.W. Daud, M.F.A. Patah, F.M. Zuki, A.S.Verdugo, Harnessing the potential of biochar-based catalysts for sustainable adsorptive and photocatalytic applications: A comprehensive review, Process Saf. Environ. Prot. 189 (2024) 387-413. https://doi.org/10.1016/j.psep.2024.05.118
[101] B. Bhattacharjee, Md. Ahmaruzzaman, Photocatalytic degradation of pharmaceuticals: Insights into biochar modification and degradation mechanism, Next Mater 5 (2024) 100238. https://doi.org/10.1016/j.nxmate.2024.100238
[102] M. Rani, U. Shanker, Degradation of traditional and new emerging pesticides in water by nanomaterials: recent trends and future recommendations, Int. J. Environ. Sci. Technol. 15 (2018) 1347 - 1380. https://doi.org/10.1007/s13762-017-1512-y
[103] S. Singh, V. Kumar, D.S. Dhanjal, S. Datta, S. Kaur, R. Romero, J. Singh, Degradation of pesticides in wastewater using heterogeneous photocatalysis. In: Shah MP (ed) Advanced Oxidation Processes for Effluent Treatment Plants, Elsevier, 2021, pp 161 - 175.
[104] J. Cui, F. Zhang, H. Li, J. Cui, Y. Ren, X. Yu, Recent Progress in Biochar-Based Photocatalysts for Wastewater Treatment: Synthesis, Mechanisms, and Applications, Appl. Sci. 10(3) (2020) 1019. https://doi.org/10.3390/app10031019
[105] F.S. Bruckmann, C. Schnorr, L.R. Oviedo, S. Knani, L.F.O. Silva, W.L. Silva, G.L. Dotto, C.R., Bohn Rhoden, Adsorption and Photocatalytic Degradation of Pesticides into Nanocomposites: A Review, Molecules 27 (19) (2022) 6261. https://doi.org/10.3390/molecules27196261
[106] J. Fito, K.K. Kefeni, T.T.I. Nkambule, The potential of biochar-photocatalytic nanocomposites for removal of organic micropollutants from wastewater, Sci. Total Environ. 829 (2022) 154648. https://doi.org/10.1016/j.scitotenv.2022.154648
[107] M. Chen, Y. Dai, J. Guo, H. Yang, D. Liu, Y. Zhai, Solvothermal synthesis of biochar@$ZnFe_2O_4$/BiOBr Z-scheme heterojunction for efcient photocatalytic ciprofoxacin degradation under visible light, Appl. Surf. Sci. 493 (2019) 1361-136. https://doi.org/10.1016/j.apsusc.2019.04.160
[108] N.T.T. Truc, D.S. Duc, D.V. Thuan, T.A. Tahtamouni, T.D. Pham, N.T. Hanh, D.T. Tran, M.V. Nguyen, N.M. Dang, C.N.T.P. Le, V.N. Nguyen, L. Chi, The advanced photocatalytic degradation of atrazine by direct Z-scheme Cu doped ZnO/g-C_3N_4, Appl. Surf. Sci. 489 (2019) 875 - 882. https://doi.org/10.1016/j.apsusc.2019.05.360
[109] M. Ismael, The photocatalytic performance of the ZnO/g-C_3N_4 composite photocatalyst toward degradation of organic pollutants and its inactivity toward hydrogen evolution: the influence of light irradiation and charge transfer, Chem. Phys. Let. 739 (2020) 136992. https://doi.org/10.1016/j.cplett.2019.136992
[110] S. Li, Z. Wang, X. Xie, G. Liang, X. Cai, X. Zhang, Z. Wang, Fabrication of vessel–like biochar–based heterojunction photocatalyst Bi_2S_3/BiOBr/BC for diclofenac removal under visible LED light irradiation: Mechanistic investigation and intermediates analysis, J. Hazzard. Mat. 391 (2020) 121407. https://doi.org/10.1016/j.jhazmat.2019.121407
[111] X. Ma, C. Ai, J. Cao, J. Li, Y. Zhu, D. Jing, Heterojunction formed by TiO_2 supported on lamellar La_2NiO_4 perovskite for enhanced visible-light-driven photocatalytic hydrogen production, J. Photon. Energy 11 (2021) 034001. https://doi.org/10.1117/1.JPE.11.034001
[112] Q.Yang, J. An, Z. Xu, S. Liang, H. Wang, Performance and mechanism of atrazine degradation using Co_3O_4/g-C_3N_4 hybrid photocatalyst withperoxymonosulfate under visible light irradiation, Colloid Physicoche. A. 614 (2021) 126161. https://doi.org/10.1016/j.colsurfa.2021.126161

[113] S. Wacławeka, H.V. Lutzeb, K. Grübele, V.V.T. Padila, M. Černíka, D.D. Dionysiou, Chemistry of persulfates in water and wastewater treatment: A review, Chem. Eng. J. 330 (2017) 44 - 62. http://dx.doi.org/10.1016/j.cej.2017.07.132
[114] T. Song, Y. Gao, J. Yang, H. Wei, Y. Jiang, Recent advances in periodate activated by carbon and carbon-doped materials in removing recalcitrant organics in water, J. Water Process Eng. 56 (2023) 104506. https://doi.org/10.1016/j.jwpe.2023.104506
[115] S. Wacławek, H.V. Lutze, K. Grübel, V.V.T. Padil, M. Černík, D.D. Dionysiou, Chemistry of persulfates in water and wastewater treatment: a review, Chem. Eng. J. 330 (2017) 44-62. https://doi.org/10.1016/j.cej.2017.07.132
[116] R. Xiao, Z. Luo, Z. Wei, S. Luo, R. Spinney, W. Yang, D.D. Dionysiou, Activation of peroxymonosulfate/persulfate by nanomaterials for sulfate radical-based advanced oxidation technologies, Curr. Opin. Chem. Eng. 19 (2018) 51 - 58. https://doi:10.1016/j.coche.2017.12.005
[117] L. Zhu, L. Tong, N. Zhao, X. Wang, X. Yang, Y. Lv, Key factors and microscopic mechanisms controlling adsorption of cadmium by surface oxidized and aminated biochars, J. Hazard. Mater. 382 (2020) 121002. https://doi.org/10.1016/j.jhazmat.2019.121002
[118] H. Zheng, J. Bao, Y. Huang, L. Xiang, B. Ren, Efficient degradation of atrazine with porous sulfurized Fe_2O_3 as catalyst for peroxymonosulfate activation, Appl. Catal. B Environ. 259 (2019) 118056. https://doi.org/10.1016/j.apcatb.2019.118056
[119] K. Khoiriah, D.V. Wellia, J. Gunlazuardi, S. Safni, Photocatalytic degradation of commercial diazinon pesticide using C, N-codoped TiO_2 as photocatalyst, Indonesian J. Chem. 20 (2020) 587 - 596. https://doi.org/10.22146/ijc.43982
[120] D. Mohanta, M. Ahmaruzzaman, A novel Au-SnO_2-rGO ternary nanoheterojunction catalyst for UV-LED induced photocatalytic degradation of clothianidin: Identification of reactive intermediates, degradation pathway and in-depth mechanistic insight, J. Hazard. Mater. 397 (2020) 122685. https://doi.org/10.1016/j.jhazmat.2020.122685
[121] H. Erdem, M. Erdem, Effect of log *Kow* on the Degradation of Pharmaceutically Active Compounds in a Heterogeneous Catalytic Persulfate Activation System, J. Environ. Chem. Eng. 12 (2024) 111720. https://doi.org/10.1016/j.jece.2023.111720
[122] A. Akbari Shorgoli, M. Shokri, Photocatalytic degradation of imidacloprid pesticide in aqueous solution by TiO_2 nanoparticles immobilized on the glass plate, Chem. Eng. Commun. 204 (2017) 1061 - 1069. https://doi.org/10.1080/00986445.2017.1337005
[123] M. Kanwal, S.R. Tariq, G.A. Chotana, Photocatalytic degradation of imidacloprid by Ag-ZnO composite, Environ. Sci. Pollut. Res. 25 (2018) 27307 – 27320. https://doi.org/10.1007/s11356-018-2693-8
[124] K. Yari, A. Seidmohammadi, M. Khazaei, A. Bhatnagar, M. Leili, A comparative study for the removal of imidacloprid insecticide from water by chemical-less UVC, UVC/TiO_2 and UVC/ZnO processes, J. Environ. Health Sci. Eng. 17 (2019) 337 – 351. https://doi.org/110.1007/s40201-019-00352-3
[125] J. Xue, J. Bao, Interfacial charge transfer of heterojunction photocatalysts: Characterization and calculation, Surf. Interfaces 25 (2021) 101265. https://doi.org/10.1016/j.surfin.2021.101265
[126] S-F. Jiang, L-L. Ling, W-J. Chen, W-J. Liu, D-C. Li, H. Jiang, High efficient removal of bisphenol A in a peroxymonosulfate/iron functionalized biochar system: Mechanistic elucidation and quantification of the contributors, Chem. Eng. J. 359 (2019) 572-583. https://doi.org/ 10.1016/j.cej.2018.11.124
[127] J. Sharma, I.M. Mishra, V. Kumar, Degradation and mineralization of Bisphenol A(BPA)in aqueous solution using advanced oxidation processes: UV/H_2O_2 and UV/$S_2O_8^{2-}$ oxidation systems, J. Environ. Manage. 156 (2015) 266-275. https://doi.org/10.1016/j.jenvman.2015.03.048
[128] T. Wang, W. Liu, L. Xiong, N. Xu, J. Ni, Influence of pH, ionic strength and humic acid on competitive adsorption of Pb(II), Cd(II) and Cr(III) onto titanate nanotubes, Chem. Eng. J. 215 - 216 (2013) 366 - 374. http://dx.doi.org/10.1016/j.cej.2012.11.029

Table 1. A review of biochar (BC)-based catalysts as activator in SR-AOPs and PI-AOPs for the free radicals driven pesticide degradation in water

No.	BC precursor	Catalyst type and properties	Process conditions	Target pesticide	Water type	Main findings	Author
1	Wheat straw	BC doped with Fe/Mn (FeMn-BC): -SSA: 186.6 m^2/g, -PV: 0.166 cm^3/g	5 mg/L TMX; Fe/Mn ratios for BC doping (1/1, 3/1, and 6/1); 0.01-1 g/L BC; 2-8 mM PS; pH 3-11; reaction time 120 min.	Thiametho-xam (TMX)	Synthetic water; tap water; river water	FeMn-BC showed excellent TMX removal efficiency (up to 99% removal in 90 min.). FeMn-BC/PS has a broad pH adaptation range, good catalytic activity and stable recoverability. TMX degradation was promoted by $SO_4^{\bullet-}$ and $HO^{\bullet}$.	Yang et al. [30]
2	Corn straw	BC codoped with N and B (BC-NB900): -SSA: 607.1 m^2/g -PV: 0.41 cm^3/g - 61.91 wt% C; 28.07 wt% O; 0.15 wt% S; 5.31 wt% N; 2.25 wt% H	10 mg/L BSM; 0.1-0.3 g/L; 0.5-2 mM PDS; pH 3-11; reaction time 120 min.; temperature 5-35 °C	Bensulfuron methyl (BSM)	Synthetic water	Graphitic N and BC_3 were identified as dominant species towards PDS activation. 92.7% of BSM removal within 30 min. under acidic and neutral pH was achieved. BC-NB900 has stable catalytic performance in the presence of various anions and reusability test.	Yang et al. [31]
3	Rice husk	N-doped BC (NBC3): -SSA: 177.13 m^2/g -PV: 0.149 cm^3/g - 56.01 % C; 11.03 % O; 8.11% N	5 mg/L DMM; Mass ratios of rice husk to urea (1:3 obtaining NBC3); 0.1-0.8 g/L; 0.5-4 mM PMS; pH 3-11; reaction time 150 min.	Dimetho-morph (DMM)	Synthetic water	N- doping reduces the adsorption capacity and improves the BC catalytic ability. Increasing the N-doping level caused the increase in catalytic removal efficiency of DMM in the presence of PMS (from 16.6% to 86.8%) with stable performance over a pH range of 3–9.	Yu et al. [16]
4	Spinach leftovers	BC derived from spinach remnants -SSA: 1.95 m^2/g -PV: 0.033 cm^3/g - 27.85 wt% C; 21.49 wt%	5-15 mg/L ATZ; 0.5-2.5 g/L BC; 3-9 mM PS; pH 3-9; reaction time 120 min.	ATZ	Synthetic water; agrochemical industrial wastewater	Efficient degradation of atrazine (99.8%) in BC/PS system was achieved with a high recyclability performance after five sequential	El-Bestawy et al. [64]

No.	BC precursor	Catalyst type and properties	Process conditions	Target pesticide	Water type	Main findings	Author
		O; 23.45 wt% K				cycles and in real wastewater system. $SO_4^{\bullet-}$ have a prime role in degrading atrazine.	
5	*Acantho-panax senticosus* (AS), medicine residue	ASBC600: -SSA: 9.0521 m^2/g	20 µM ATZ; 0.01-0.05 g/L ABSC600; 20-200 kHz US; 0.2-3 mM PMS; pH 3-7; reaction time 50 min.	ATZ	Distilled water; river water; tap water	70% of ATZ degradation was achieved within 50 min. using ASBC600/US/PMS system, primarily promoting the formation of $SO_4^{\bullet-}$ and $HO^{\bullet}$. Synergism of US and ASBC for the PMS activation was observed.	Jia et al. [65]
6	Rice husk	P-doped activated C-supported trace cobalt ferrite composit (PCoFe@BC_5): -SSA: 450.99 m^2/g -PV: 0.49 cm^3/g - 69.82 wt% C; 17.32 wt% O; 8.49 wt% P; 2.18 wt% Co; 2.19 wt% Fe	20 mg/L 2,4-D; 0.03-0.2 g/L; 0.1-1.5 mM PMS; pH 2-12; reaction time 60 min.; 10-40ºC	2,4-dichlorophenoxyacetic acid (2,4-D)	Deionized water	P-CoFe@BC_5/PMS oxidation system proved to be highly effective in degrading 2,4-D within 60 min. (98.3%, with strong performance within wide pH range of 2-10. Free and non-free radicals pathway was included in the degradation.	Liang et al. [66]
7	Soybean stalks	BC supported sulfurized nZVI (S-nZVI@BC): -47.3 wt % C; 12 wt% O; 2.1 wt% S; 38.5 wt% Fe	10 mg/L ATZ; 0-0.3 S/Fe; 0.05-0.25 g/L S-nZVI@BC; 0.5-2 mM PS; pH 2.86-10.53; reaction time 60 min.; 15-35ºC	ATZ	Deionized water; Tap water; River water	BC support and S-doping improve the stability of nZVI. Under the optimal conditions (0.15 S/Fe; 0.1 g/L S-nZVI@BC; 1 mM PS) high ATZ removal rate (96.8%) was achieved. S-nZVI@BC exhibits a good activity after three cycles and in a wide pH range of 2.9–10.5.	Jiang et al. [67]
8	Dried wood pulp	N-doped BC-loaded nZVI composites (Fe@N_2-BC): -SSA: 214 m^2/g -PV: 0.1295	10 mg/L γ-HCH; 0-0.5-1.25 g/L Fe@N_2-BC; 2-6 mM PS; pH 3-11; reaction time	Lindane (γ-HCH)	Deionized water	Fe@N2-BC900 showed excellent catalytic performance in activating PS for γ-HCH removal (95.9% within 60	Huang et al. [68]

No.	BC precursor	Catalyst type and properties	Process conditions	Target pesticide	Water type	Main findings	Author
		cm^3/g - 38.2 at% C; 50 at% Fe; 7.47 at% O; 3.03 at% N; 1.37 at% H	180 min.; 25±1ºC			min). The N-doped defects in BC and loading of nZVI greatly enhance the PS activation and γ-HCH degradation over a wide pH range.	
9	Tobacco stem	Double modified BC with polyacrylic acid (BC_{PAA}@CFO): -SSA: 6.25 m^2/g - 51.1% C; 24.7 % O; 14.4 % Fe; 6.2 % Co; 3.7% S	5-15 mg/L QNC; 0.02-0.15 g/L BC_{PAA}@CFO; 2-6 mM PMS; pH 2-6; reaction time 4h; 25ºC	Quinclorac (QNC)	Distilled water; irrigation water (Xiangjiang and Xunlong River)	High degradation efficacy of QNC (89.96%) using BCPAA@CFO was achieved and 80.7% of removal in QNC-Pb^{2+} composite system. BCPAA@CFO composite has excellent degradation performance in actual irrigation water.	Li et al. [36]
10	Municipal dehydrated sewage sludge	Fe/Mn-SBC: -SSA: 6.2 m^2/g - 38.65 at% C; 16.50 at% O; 5.79 at% Si; 23.32 at% Fe; 2.92 at% Mn	10 mg/L TCP; 0.1-2 g/L Fe/Mn-SBC; 0.5-5 mM PI; pH 3-11; reaction time 90 min.; 25ºC	Thiacloprid (TCP)	Deionized water; tap water; lake water	TCP removal rate above 92% could be maintained in a wide pH range of 3–11 and 80% in tap and lake water by Fe/Mn-SBC/PI system. $IO_3^•$ and $^•OH$ were main free radicals in the Fe/Mn-SBC/PI system with enhanced electron transfer between iron and manganese oxides.	He et al. [69]
11	Poplar sawdust	Magnetic FeS@BC (MFB), MFB-500: - 58.44 % C; 14.04 % O; 19.53 % Fe; 7.99 % S	10 mg/L 2,4-D; 0.1-1 g/L MFB-500; 0.25-2.6 mM PMS; pH 3-10; reaction time 60 min.	2,4-D	Deionized water	MFB-500 is an effective activator of PMS for the degradation of 2,4- D with longer lifetime. Degradation of 2,4-D gradually decreased with the increasing of the initial pH; HCO_3^- and $H_2PO_4^-$ exhibit significant inhibitory effect.	Hong et al. [70]

No.	BC precursor	Catalyst type and properties	Process conditions	Target pesticide	Water type	Main findings	Author
12	Rice husk	Flakelike Co_3O_4 loaded on rice husk BC (CBC-1): -SSA: 77.04 m^2/g	10-50 mg/L 2,4-D; 0.05-0.3 g/L CBC-1; 0.4-1.2 mM PMS; pH 3-11; reaction time 10 min.; 10-40ºC.	2,4-D	Deionized water	The incorporation of BC improves the formation of the morphological Co_3O_4 nano-sheet structure and catalytic performance. Accelerated electron transfer and active free radical generation cause effective 2,4-D degradation within three cycles.	Liang et al. [71]
13	Soybean stalks	nZVI@BC800: - 65.1 % C; 8.3 % O; 1.6 % N; 25 % Fe	10 mg/L ATZ; 0.1-0.5 g/L nZVI@BC; 0.5-1.5 mM PS; pH 0-12; reaction time 30 min.	ATZ	Distilled water; Tap water; River water	nZVI@BC composite could effectively activate PS promoting the effective oxidative degradation of atrazine (up to 93.8%), with a wide pH tolerance range. ATZ degradation decreased in tap water (75%) and river water (35%).	Zhang et al. [72]
14	Leaves of *Lagerstro-emia speciose*	CuO, CuO/BC, pyrite; CuO/BC: - 59.60 % C; 10.96 % O; 0.48 % S; 37.87 % Cu	30 mg/L IMI; 1 g/L CuO/BC; 0.5 mM SPS; pH 3-11; reaction time 300 min.	Imidacloprid (IMI)	Deionized water, Tap water; Urban sewage water	BC-support did not increase the CuO activation efficiency. IMI degradation efficacy can be summarized as CuO/BC-SPS < CuO-SPS < PyR-SPS. Highest IMI degradation by CuO-SPS and CuO/BC-SPS was achieved over pH 11.0.	Hayat et al. [73]
15	Corn stalks	ZVI/BC: -SSA: 68.075 m^2/g - PV: 0.043 cm^3/g - 63.31 wt% C; 6 wt% O; 31 wt% Fe	25 mg/L ATZ; 0.05-0.175 g/L ZVI/BC; 0.6-2 mM PS; pH 3-8; reaction time 30 min.	ATZ	Deionized water	Effective atrazine removal (83.77%) can be achieved using ZVI/BC-PS system. ZVI/BC activated PS producing $SO_4^{\cdot-}$ and $HO^{\cdot}$ which accompany with the iron valent changing causing ATZ degradation.	Jiang et al. [34]
16	Sludge from a	Sludge-derived	10 mg/L TCS; 0.1-	Triclosan (TCS)	Distilled water;	SBC-PMS system under optimal	Wang and

No.	BC precursor	Catalyst type and properties	Process conditions	Target pesticide	Water type	Main findings	Author
	municipal sewage treatment plant	biochar (SBC): -SSA: 157.4 m^2/g - 59.9 % C; 30.3 % O; 8,7 % N; 0,7 % Mg; 0.5 % Fe.	1 g/L SBC; 0.2-1.2 mM PMS; pH 3.2-9.4; reaction time 240 min., 15-35 ºC.		Domestic wastewater	conditions (pH 7.2, 1.0 g/L SBC, 0.8 mM PMS, 25 °C) provide 99.2% of TCS removal. TCS degradation occurred via hydroxyl and sulfate radicals and singlet oxygen contribution.	Wang [74]
17	Rice straw	Magnetic N-doped BC supported $CoFe_2O_4$ composite, $MNBC_{800}$: -SSA: 150.7 m^2/g -PV: 0.081 cm^3/g -76.4 % C; 20.2 % O; 1.53 % N.	10 mg/L MET; 0.2 g/L $MNBC_{800}$; 0.1-3 mM PMS; pH 3-11; reaction time 40 min.	Metolachlor (MET)	Wastewater; River water; Groundwater	The degradation process by $MNBC_{800}$-PMS was pH-dependent and favourable at neutral and weak basic conditions. MET degradation was moderately and significantly inhibited in groundwater and wastewater. MET catalytic degradation occurred via both radical and non-radical pathway.	Liu et al. [75]

Table 2. A review of BC-based catalysts as activator in SR-AOPs and PI-AOPs for the free radicals driven pesticide intermediate compounds degradation in water

No.	BC precursor	Catalyst type and properties	Process conditions	Target pesticide	Water type	Main findings	Author
1	Biomass (bagasse)	Fe/Mn-BC	0.5 - 5 g/L catalyst; 1-10 mM PDS; pH 3-11; temperature 30°C; reaction time 30 min.	2,4-dichloro-phenol (2,4-DCP)	Synthetic water	83.7% of 2,4-DCP removal within 30 min. was achieved. $SO_4^{\bullet-}$ and $HO^{\bullet}$ generated by Fe/Mn-BC-activated PDS have similar contribution to the 2,4-DCP degradation.	Zhang et al. [76]
2	Sawdust of birch tree	BC co-doped with N and S (NS-BC) -SSA: 2183.75 m^2/g	50-100 mg/L 4-CP; N/S ratio (3:0.25; 3:0.5; 3:0.75 and 3:1); 0.02-	p-chloro-phenol (4-CP)	Wastewater	N-BC and S-BC performance was more superior than pure BC, but less effective compared to double	Zhong et al. [77]

No.	BC precursor	Catalyst type and properties	Process conditions	Target pesticide	Water type	Main findings	Author
			0.08 g/L NS-BC; 0.25-0.5 mM PMS, reaction time 30 min.			doping (NS-BC). Complete degradation 4-CP was achieved within 30 minutes (N/S ratio 3:0.5 and 0.5 mM PMS).	
3	Sludge	Fenton sludge(FS)-BC: -SSA: 19.87 m^2/g; -PV: 0.16 cm^3/g; -1.53 wt% C; 0.35 wt% H; 0.04 wt% N. Sewage sludge (SS)-BC: -SSA: 71.09 m^2/g; -PV: 0.31 cm^3/g; -36.89 wt% C; 1.52 wt% H; 1.01 wt% N	Catalyst dosage 0.4-1.4 g/L; SS:FS mass ratio from 1:1 to 9:1; 1.56-4.69 mM PDS; temperature 15-45°C; pH 2-12; reaction time 60 min.	1-H-1,2,4-triazole (TZ)	Deionized water	96.7% of TZ degradation was achieved within 60 min. SS:FS-5:1BC/PDS system displayed significant resistance to temperature, pH, and the presence of NOM and co-existing ions. $SO_4^{\bullet-}$ exhibiting the highest degradation efficacy, followed by $HO^{\bullet}$, $O_2^{\bullet-}$ and $^1O_2$.	Tong et al. [78]
4	Peanut shells	Magnetic Fe_3S_4/BC: -40.58 wt % C; 6.23 wt % O; 34.31 wt % S and 18.88 wt % Fe	5-40 mg/L 2,4,6-TCP; 0.2-1.0 g/L Fe_3S_4/BC; 0.2-1.0 mM PMS; HA 1-10 mg/L; pH 3-11; temperature 15-35°C; reaction time 60 min.	2,4,6-trichloro-phenol (2,4,6-TCP)	Deionized water	The catalytic performances of Fe_3S_4/BC were improved compared to the pure Fe_3S_4. 2,4,6- TCP can be completely degraded within 60 min under optimal conditions with a primary role of $SO_4^{\bullet-}$ and $HO^{\bullet}$.	Li et al. [37]
5	/	Commercial BC: -SSA: 459 m^2/g; - 90 wt % C	10 mg/L phenol; 0.1-1.0 g/L BC; 0.5-5.0 mM PS; 10, 20 and 40 mM of Cl^-, HCO_3^-, HPO_4^{2-} and NO_3^-; HA 1-20 mg/L; pH 3-9; reaction time 120 min.	Phenol	Distilled water	Phenol can be completely removed within 120 min. (1 mM PS, 0.25 g/L BC and pH of 5.2). The presence HA has a strong inhibitory effect $HO^{\bullet}$ play a more substantial role compared to $SO_4^{\bullet-}$ in the radical pathway, whereas $^1O_2$ predominates in the non-radical pathway.	Miserli et al. [79]
6	Rice husk	Magnetic $CoFe_2O_4$@BC	p-NCB 10 mg/L; 0.1 g/L $CoFe_2O_4$@BC; 1 mM PMS, reaction time 240 min.	p-nitro-chlorobenze-ne (p-NCB)	Synthetic water	$CoFe_2O_4$@BC/PMS system removes 89% of p-NCB within 240 min. The synergistic effect of iron and cobalt in composite enhances electron transfer, promoting the ROS generation including $SO_4^{\bullet-}$, $HO^{\bullet}$, $O_2^{\bullet-}$ and $^1O_2$.	Zhi et al. [80]
7	Peanut	nZVI/BC:	5-20 mg/L	Nitrochloro-	Synthetic	The initial concentration	Wang

No.	BC precursor	Catalyst type and properties	Process conditions	Target pesticide	Water type	Main findings	Author
	shell	-SSA 6.3 m^2/g; - 61.3 wt % C, 2.69 wt % H, 12 wt % O, 1.66 wt % N.	NCB; mass ratio nZVI/BC (1:1 and 1:4); 0.005-0.02 g/L nZVI/BC; reaction time 120 min.	benzene (NCB)	water	of NCB had a negligible impact on the degradation. Over 90% removals of three NCB isomers was obtained under optimal conditions within 120 min.	et al. [81]
8	Green tea	Green (G-) nZVI-BC and traditional C-nZVI-BC	10 mg/L PNP; mass ratio nZVI/BC (0.2:1-1:1); 0.2-1.6 g/L G-nZVI-BC; PDS/PNP molar ratio 10:1-400:1; pH 2.15-9.23; reaction time 90 min.	p-nitro-phenol (PNP)	Synthetic water, surface water; ground-water	G-nZVI-BC/PDS system was more resistant to oxidation of PNP than the C-nZVI-BC/PDS. G-nZVI-BC/PDS system has shown effectiveness in removing PNP across a wide pH range (pH 3.06-9.23).	Wang et al. [82]
9	Rice straw (RS)	nZVI/RS500: -SSA: 15.5 m^2/g	20-100 μM MCB; mass ratio nZVI/RS (1:1); 0.025-0.5 g/L nZVI/RS500; 0.5-12 mM PS; pH 3-11; temperature 25°C; reaction time 180 min.	Monochloro-benzene (MCB)	Synthetic water; groundwa-ter; tap water	The most efficient removal of MCB (98.8%) was observed in the nZVI/RS500-PS system. The lower removal efficiency of MCB was obtained in tap water and groundwater than in ultrapure water (67.4-80.2%).	Yang et al. [83]
10	Grapefruit peel	Magnetic biochar supported MnO_2 composite (MBM); SSA 83.405 m^2/g; 45.27 wt % C, 38.75 wt % O, 0.76 wt % K, 10.38 wt % Mg, 4.85 wt % Fe.	Mass content of MnO_2 in MBM was 25, 50 and 75%; 5-20 mg/L 4-CP; 0.1-0.4 g/L MBM; pH 3-9; reaction time 180 min.	4-chloro-phenol (4-CP)	Ultrapure water	Activation of PDS through MBM generates mainly the singlet oxygen, which could be response for the mineralization of 4-CP. Complete removal of 4-CP was achieved when the applied of MBM-50 catalyst in the neutral medium.	Zhou et al. [84]
11	Wheat straw (WSH), chicken manure (CMC) and rice husk (RHC)	WSH: SSA 29.80 m^2/g. Atomic %: 57.68% C, 3.11% H, 0.89% N, 1.42% S, 14.94% O, 0.001% Cu, 0.047% Mg, 0.023% Fe, 0.329% Ca, 0.181% Na, 0.657% K. CMC: SSA 5.57 m^2/g. 43.05% C, 2.10% H, 3.49% N, 2.37% S,	10 mg/L PNP; 0.8 g/L BC; 10 mM PS; temperature 25°C, pH 4.4-10.4; reaction time 840 min.	p-nitro phenol (PNP)	Synthetic water	RHC exhibited the best adsorption performance. Adding of PS resulted in improvement in the removal of PNP, indicating the presence of a synergistic effect within the BC/PS combination. Over 80% of PNP was removed in the RHC/PS system.	Chenfei et al. [85]

No.	BC precursor	Catalyst type and properties	Process conditions	Target pesticide	Water type	Main findings	Author
		9.72% O, 0.019% Cu, 1.734% Mg, 0.271% Fe, 4.544% Ca, 1.582% Na, 3.903% K. RHC:SSA 126.87 m^2/g. 53.34% C, 2.72% H, 0.64% 0.022% Mg, 0.021% Fe, 0.132% Ca, 0.056% Na, 0.151% K.					
12	Sludge	Sludge-derived biochar (SDBC)/ PS SSA: 70.12 m^2/g; PD: 7.947 nm	SDBC dosage from 0.2-1.2 g/L; 4-CP 10 mg/L; PS 0.74-18.50 mM; pH 3-9.4; temperature 25°C; reaction time 100 min.	4-chloro-phenol (4-CP)	Deionized water; Real wastewater	In deionized water was achieved the removal of 4-CP of 92.3% under optimal conditions. In real wasterwater, 56.0% of TOC and 98.7% of ammonia was removed by SDBC/PS system after 12 h reaction with 5 g/L SDBC and 150 mM PS.	Wang et al. [86]

Table 3. A review of BC-based photocatalysts for degradation of pesticide and its intermediates in water

No.	BC precusor	Photocatalyst type and properties	Process conditions	Target pesticide	Water type	Main findings	Authors
1.	Reed	γ-Fe_2O_3/BC (BFγ) - SSA 38.24 m^2/g -PV 0.183 cm^2/g	20 mg/L p-chlorphenol; 0.2 g/L BFγ; pH 6.1; irradiation source: xenon arc lamp; irradiation time 120 min	p-chlorophenol (4-CP)	Synthetic water	The degradation efficiency of 4-CP reached 96.4% in 120 min in BFγ/PMS/Vis system.	Zhang et al. [87]
2.	Grapefruit skin	BC/CdS-Fe_3O_4: -9.80 wt % C; 20.70 wt % O; 35.20 wt % Fe; 30.1 wt % Cd; 4.2 wt % S	0.002-0.008 mg/L chlorpyrifos; 10-20 g/L BC/CdS-Fe_3O_4; pH 3-11; irradiation source: visible LED light; irradiation time 90 min.	Chlorpyrifos	Synthetic water	Efficient degradation of chlorpyrifos (97%) was achieved by BC/CdS-Fe_3O_4 . The photocatalytic activity was dependent on time, pH, pesticide concentration, and was good after 7 cycles (81%).	Farahba-khsh et al. [45]
3.	The stalks of the raw date	3D-TiO_2/magnetic BC dots (3D-TiO_2/BCDs MNPs)	20-150 mg/L diazinon; 0.1-0.5 3D-TiO_2/BCDs MNP_S; pH 2-	Diazinon	Distilled water	The 3D-TiO_2/ BCDs MNPs displayed high performance for diazinon	Zahedi-far and Seyedi [88]

No.	BC precusor	Photocatalyst type and properties	Process conditions	Target pesticide	Water type	Main findings	Authors
			11; irradiation source: sunlight; irradiation time 90 min.			degradation of 98.5% in 30 min under sunlight irradiation. The 3D-TiO_2/ BCDs MNPs showed an excellent recoverability without losing the magnetic properties after five runs.	
4.	Rice straw	Core–shell P-laden BC/ZnO/g-C_3N_4 composite (Pbi-ZnO-g-C_3N_4): SSA: 17.5 m^2/g	10 mg/L ATZ; 0.1 g/LPbi-ZnO-g-C_3N_4; pH 7; irradiation source: xenon arc lamp; irradiation time 260 min.	ATZ	Synthetic water	Pbi-ZnO-g-C_3N_4 exhibits enhanced photocatalytic activity with the maximum ATZ degradation efficiency of 85.3% after 260 min. Formation of Z-scheme heterojunction between ZnO and g-C_3N_4 promoted the separation of electron-hole pairs.	An et al. [89]
5.	Rice straw	BC-supported α-Fe_2O_3/MgO composite (BC-α-Fe_2O_3/MgO): -SSA 35.2 m^2/g - 50.36 wt % C; 29.30 wt % O; 12.28 wt % Mg; 6.98 wt % Fe	10 mg/L NPA; 0.5 g/L BC-α-Fe_2O_3/MgO; pH 8.5; irradiation source: xenon arc lamp; irradiation time 80 min.	N-phosphonomethyl iminodiacetic acid (NPA)	Synthetic water	The degradation efficiency of NPA by BC-α-Fe_2O_3/MgO reach 90.1%, providing a high stability during five cycling experiments. Holes, $HO^{\bullet}$, and $^{\bullet}O_2^-$ radicals generated in the photocatalytic process are responsible for NPA degradation.	An et al. [90]
6.	-	Commercial BC: SSA: 459 m^2/g	10 mg/L MBZ; 0.05-0.4 g/L BC; pH 7; irradiation source: xenon arc lamp; irradiation time 180 min.	Metribuzin (MBZ)	Synthetic water	Low concentration of BC (0.05 g/L) effectively photodegradate MBZ (91%). $HO^{\bullet}$ and $^1O_2$, photogenerated by BC, are the main reactive intermediates.	Serelis et al. [91]
7.	Rice husk	TiO_2 nanoparticles are immobilized BC	15 mg/L glyophosphat	Glyphosate	Synthetic water	The photodegradatio	Le et al. [92]

No.	BC precusor	Photocatalyst type and properties	Process conditions	Target pesticide	Water type	Main findings	Authors
		(TiO_2/RHB)	e; 3-20 g/L TiO_2/RHB; pH 3; irradiation source: light source with emission at 365 nm; irradiation time 300 min.			n efficiency of glyphosate was up to 99% after 5 h of irradiation (pH 3.0, 10 g/L TiO_2/RHB). Synergetic relationship between TiO_2 and BC was observed.	
8.	Pruning waste of *Prunus dulcis*	BC supported ternary g-C_3N_4/$Bi_2O_2CO_3$/$CoFe_2O_4$ heterojunction (BCBF) -SSA: 68.24 m^2/g	20 mg/L PQT; 0.5 g/L BCBF; pH 3-11; irradiation source: xenon arc lamp; irradiation time 90 min.	Paraquat (PQT)	Distilled water	BCBF shows high PQT degradation of 99.3% under visible radiation in 90 min and 92.1% under solar light in 120 min. BCBF catalyst shows a promising photo-reduction of CO_2 into CH_4.	Kumar et al. [93]
9.	Maple and oak woodlands	TiO_2 (or ZnO) and BC: - 75.8 wt %C; 0.90 wt %N; 84.2 C/N	1.93 mg/L FRS; 0.25 g/L BC and 2.5 g/L TiO_2 (or ZnO); pH 6.1-6.7; irradiation source: four black light fluorescent (λ= 365 nm); irradiation time 120 min.	Foramsulfuron (FRS)	Distilled water	The photodegradation mediated by TiO_2 or ZnO mineralized entirely the herbicide. BC presence in FRS solution containing TiO_2 or ZnO did not affect the FRS photodegradation rate.	Pinna et al. [94]

Table 4. Results of the meta analysis of investigated AOPs

Group	Subgroup	Random effects model results				Heterogeneity		
		WDE (%)	Lower CI (%)	Upper CI (%)	n	Q	I^2 (%)	p
SR-AOPs and PI-AOPs								
Catalyst type	pristine	90	79	101	8	690	99	0.0145
	metal or non-metal doped BC	91	83	99	16	380	96	
	metal and non-metal doped BC	99	98	100	7	20.9	71	
Overall		92	88	97	31			
Oxidant type	PS	92	85	98	20	390	95	0.1979
	PMS	89	78	100	1	881	99	

					1			
	PI	96	96	96	1	-	-	
Overall		91	86	96	32			
pH	pH <5	82	73	91	31	66830	100	0.0207
	pH 5-8	86	80	92	31	128809	100	
	pH ≥9	70	60	80	33	63304	100	
Overall		79	74	84	95			
Type of pesticides/ intermediates	Triazine and triazole	91	76	106	6	672	99	0.0385
	Neonicotinoids	77	-10	165	3	212	99	
	Sulfonylurea	99	99	99	1	-	-	
	Organochlorine and other chlorinated compounds	97	94	100	8	54.9	87	
	Intermediates	93	90	97	13	176	93	
Overall		93	88	97	31			
Water matrix	Deionized or distiled (synthetic)	93	89	97	32	1017	97	0.0016
	Tap water	80	53	108	5	1736	100	
	Natural water	80	63	97	9	1946	100	
	Wastewater	63	34	90	7	4979	100	
	Chloride (1-10 mM)	73	51	94	10	117708	100	
	Nitrate (1-10 mM)	82	54	110	7	1964	100	
	Carbonate (1-10 m)	66	46	86	10	4483	100	
	Humic acids (5-10 mg/L)	84	72	95	9	1598	100	
	Humic acids (10-50 mg/L)	71	27	115	5	1238	100	
Overall		81	76	86	94			
Photocatalysis								
Photocatalyst type	pristine	91	91	91	1	-	-	0.726
	metal doped BC	91	81	100	6	104.0	95	
	metal and non-metal doped BC	95	74	116	3	14.6	86	
Overall		92	88	97	10			
pH	(1) pH ≤ 5	78	65	92	8	253	16	0.2446
	(2) pH 5-8.5	83	75	92	14	233	15	
	(3) pH ≥9	62	27	97	5	794	28	
Overall		78	70	86	27			

Table 5. Summary of pesticides and intermediate compound degradation mechanism and pathways during the biochar-based catalysts AOPs

Target compound	Oxidation system and main reactive species	Degradation pathway	Transformation intermatiates	Ref.
ATZ	$\xrightarrow{BC/PS[SO_4^{\bullet-}]}$	Side-chain oxidation, dechlorination, isomerization, ring cleavage	m/z 146; 128; 198; 196; 133; 74	[64]
	$\xrightarrow{ASBC600/US/PMS\ [SO_4^{\bullet-},HO^{\bullet}]}$	Dichlorohydroxylation and non-dichlorohydroxylation pathways, hydrolysis, alkyl-hydroxylation, alkyl-oxidation, olefination, dealkylation	m/z 230; 214; 212; 202; 198; 196; 174; 172; 146; 126	[65]
	$\xrightarrow{S-nZVI@BC-PS\ [HO^{\bullet},SO_4^{\bullet-},1_{O_2}]}$	Dechlorination, alkyl-oxidation, dealkylation, olefination	m/z 190, 146, 130; 128	[67]
	$\xrightarrow{nZVI@BC-PS\ [SO_4^{\bullet-},HO^{\bullet},PFRs,1_{O_2}]}$	Alkyl-oxidation, dealkylation, dehydrogenation, dechlorination hydroxylation, olefination	m/z 190; 230; 214; 188; 172; 212; 170; 128	[72]
	$\xrightarrow{ZVI/BC-PS\ [SO_4^{\bullet-},HO^{\bullet}]}$	Dealkylation, alkyl oxidation and dechlorination-hydroxylation	m/z 198; 230; 212; 188; 180; 146; 128	[34]
	$\xrightarrow{Pbi-ZnO-g-C_3N_4/Xe\ lamp\ [HO^{\bullet},O_2^{\bullet-}]}$	Olefination and dichlorination, carbonylation, hydroxylation, dealkylation, alkylic-oxidation; deamination-hydroxylation and carboxyl ammoniation, mineralization	m/z 232; 230; 212; 198; 196; 170; 146; 126	[89]
TZ	$\xrightarrow{SS:FS-5:1BC/PDS\ [SO_4^{\bullet-},HO^{\bullet},O_2^{\bullet-},1_{O_2}]}$	Introduction of hydroxyl groups, oxidation into carbonyl and carboxyl group, decarboxylation and ring cleavage; deamination pathways	1H-1,2,4-triazol-5-ol; 2,4-dihydro-3H-1,2,4-triazol-3-one; (Z)-hydrazonomethyl carbamic acid; Carbamimidic acid; (Z)-formohydrazonic acid	[78]
TMX	$\xrightarrow{FeMn-BC/PS\ [SO_4^{\bullet-},HO^{\bullet}]}$	Generation of hydroxyl groups and the cleavage of the methylamine group	m/z 274; 306; 263; 279; 260; 232; 247; 248; 163; 135; 117; 118	[30]
TCP	$\xrightarrow{Fe/Mn-SBC/PI\ [HO^{\bullet},IO_3^{\bullet}]}$	Hydroxylation, oxidation, cyano hydrolysis and chloropyridinyl dichlorination	m/z 269; 285; 301; 267; 240; 256	[69]
BSM	$\xrightarrow{BC-NB900/PDS\ [1_{O_2},\ SO_4^{\bullet-},HO^{\bullet},O_2^{\bullet-}]}$	Cleavage of sulfonylurea bridge, sulfonyl amide linkage and C-N bond	m/z 156; 252; 198	[31]
DMM	$\xrightarrow{NBC3/PMS\ [SO_4^{\bullet-},\ 1_{O_2},\ HO^{\bullet},O_2^{\bullet-}]}$	Hydroxylation, dechlorination, and dealkylation	m/z 276; 87; 353; 373; 403; 208; 282	[16]
2,4-D	$\xrightarrow{P-C_0Fe@BC_5/PMS\ [1_{O_2},SO_4^{\bullet-},O_2^{\bullet-},HO^{\bullet}]}$	Decarboxylation, substitution and ring cleavage	m/z 194; 176; 160; 143; 115	[66]
TCS	$\xrightarrow{SBC/PMS\ [SO_4^{\bullet-},HO^{\bullet},\ 1_{O_2}]}$	Dechlorination and hydroxylation	m/z 233, 248, 197, 165 and 181	[74]

MET	$\xrightarrow{MNBC_{800}/PMS\ [SO_4^{\bullet-},HO^{\bullet},1_{O_2}]}$	Hydroxylation, dechlorination, and dealkylation	m/z 265; 269; 24; 249; 207; 237; 213; 211; 179; 135; 151	[75]
2,4,6-TCP	$\xrightarrow{Fe_3S_4/BC/PMS\ [SO_4^{\bullet-},HO^{\bullet}]}$	Dechlorination, hydroxylation, oxidation, ring cleavage	2,4-dichlorophenol; 2,6- dichlorophenol; 2,6-dichlorohydroquinone; 3,5-dichlorocatechol; 2,6-dichloro-1,4-benzoquinone; 3,5-dichloro-1,2-benzoquinone; 2,3,4,6-tetrachlorophenol; 2,6-dichloro-3-hydroxy-1,4-benzoquinone	[37]
4-CP	$\xrightarrow{NS-BC/PMS\ [O_2^{\bullet-},\ 1_{O_2}]}$	Dechlorination, oxidation, ring opening, carboxylic acid formation and mineralization[77,84,87]	m/z 195;97; 127;116	[77]
	$\xrightarrow{MBM/PDS\ [1_{O_2}]}$		m/z 143	[84]
	$\xrightarrow{BF\gamma/PMS/Vis\ [h^+,e^-,SO_4^{\bullet-},HO^{\bullet},O_2^{\bullet-},1_{O_2}]}$		m/z 143; 123; 94; 109; 107; 115; 89; 74, 60	[87]
p-NCB	$\xrightarrow{CoFe_2O_4@BC/PMS\ [SO_4^{\bullet-},\ HO^{\bullet},O_2^{\bullet-}]}$	Dechlorination, denitrification and hydroxylation, ring opening and mineralization	m/z173; 129; 110; 162; 139; 108; 155	[80]
PNP	$\xrightarrow{G-nZVI-BC/PDS\ [SO_4^{\bullet-},O_2^{\bullet-}]}$	Polyhydroxy compounds formation, ring opening, generating carboxylic acids, mineralization	m/z 110; 108; 98; 94	[82]
MCB	$\xrightarrow{nZVI/RS500-PS\ [SO_4^{\bullet-},HO^{\bullet},O_2^{\bullet-}]}$	Electron transfer, hydrolysis, hydroxyl substitution, oxidation, ring opening, mineralization	Phenol; p-chlorophenol; o-chlorophenol; oxalic acid; glycolic acid; acetic acid	[83]
NPA	$\xrightarrow{BC-\alpha-Fe_2O_3/MgO/Xe\ lamp\ [h^+,HO^{\bullet},O_2^{\bullet-}]}$	Formation of phosphate, sarcosine, and aminomethylphosphonic acid, decarboxylation, mineralization	m/z 88; 111; 230; 74; 30; 46; 94	[90]
Glyphosate	$\xrightarrow{TiO_2/RHB/UV\ [na]}$	Formation of aminomethylphosphonic acid and orthophosphate ions	AMPA; orthophosphate	[92]
PQT	$\xrightarrow{BCBF/Xe\ lamp\ [HO^{\bullet},O_2^{\bullet-}]}$	Oxidation by HO·, hydrolysis, ring opening and mineralization	m/z 203; 173; 156; 138; 90; 74	[93]

Declarations

Competing interests: The authors do not have any competing interests.

Highlights:

- Biochar-based catalyst boosts the pesticides/intermediates degradation by AOP.
- Overall WDE was 92% in SR-AOP and PI-AOP, and photocatalysis.
- Degradation efficacy decreased in alkaline conditions (pH≥9).
- WDE dropped in wastewater < hydrogencarbonate (1-10 mM) < humic acids (10-50 mg/l).
- Biochar catalysts have the groundbreaking potential in micropollutants abatement over wide pH.